Deciphering competitive interactions: Phosphate and organic matter binding on goethite through experimental and theoretical insights

Ashour A. Ahmed[a,*], Mohsen Morshedizad[b], Oliver Kühn[a], Peter Leinweber[b]

[a] Institute of Physics, University of Rostock, Albert-Einstein-Str. 23-24, D-18059 Rostock, Germany

[b] Chair of Soil Science, University of Rostock, Justus-von-Liebig-Weg 6, D-18059 Rostock, Germany

Corresponding Author: Ashour A. Ahmed (ashour.ahmed@uni-rostock.de)

Abstract

The adsorption of phosphorus (P) onto active soil surfaces plays a pivotal role in immobilizing P, thereby influencing soil fertility and the filter function of soil to protect freshwater systems from eutrophication. Competitive anions, such as organic matter (OM), significantly affect the strength of this P-binding, eventually controlling P mobility and release, but surprisingly, these processes are insufficiently understood at the molecular level. In this study, we provide a molecular-level perspective on the influence of OM on P binding at the goethite-water interface using a combined experimental-theoretical approach. By examining the impact of citric acid (CIT) and histidine (HIS) on the adsorption of orthophosphate (OP), glycerolphosphate (GP), and inositol hexaphosphate (IHP) through adsorption experiments and molecular dynamics simulations, we address fundamental questions regarding P binding trends, OM interaction with the goethite surface, and the effect of OM on P adsorption. Our findings reveal the complex nature of P adsorption on goethite surfaces, where the specific OM, treatment conditions (including covering the surface with OM or simultaneous co-adsorption), and initial concentrations collectively shape these interactions. P adsorbs on goethite with an order of GP < OP < IHP. Crucially, this trend remains consistent across all adsorption experiments, regardless of the presence or absence of OM, CIT, or HIS, and irrespective of the specific treatment method. Notably, OP is particularly susceptible to inhibition by OM, while adsorption of GP depends on specific OM treatments. Despite being less sensitive to OM, IHP shows reduced adsorption, especially at higher initial P concentrations. Of significance is the strong inhibitory effect of CIT, particularly evident when the surface is pre-covered, resulting in a substantial 70% reduction in OP adsorption compared to bare goethite. The sequence of goethite binding affinity to P and OM underscores a higher affinity of CIT and HIS compared to OP and GP, suggesting that OM can effectively compete with both OP and GP and replace them at the surface. In contrast, the impact of OM on IHP adsorption appears insignificant, as IHP exhibits a higher affinity than both CIT and HIS toward the goethite surface. The coverage of goethite surfaces with OM results in the blocking of active sites and the generation of an unfavorable electric potential and field, inhibiting anion adsorption and consequently reducing P binding. It is noteworthy that electrostatic interactions predominantly contribute more to the binding of P and OM to the surface compared to dispersion interactions.

Keywords: Phosphates, P adsorption, P binding, Mineral surfaces, Molecular modeling, MD simulations

1. Introduction

Phosphorus (P) is indispensable for all life forms, and its efficient utilization in fertilizers is essential for sustaining a rapidly growing human population (Maciá, 2005). The affinity of soil for P adsorption, alongside the capacity and strength of this process, significantly influences P immobilization. This significantly affects soil fertility and the fate of P in natural environments such as transfer from soil to freshwater systems, where P accelerates eutrophication (Ahmed et al., 2023; Andersen et al., 2015; Roy et al., 2017; Tisdale and Tisdale, 1993; Y. T. Wang et al., 2016). These aspects are significantly influenced by the diverse interactions of P with soil constituents involving free metal ions (Gros et al., 2019; Urrutia et al., 2013), soil minerals (Ahmed et al., 2019; Ganta et al., 2021; Kruse et al., 2015; Kubicki et al., 2012; Liu et al., 2022), and soil organic matter (Ahmed et al., 2018a; Debicka et al., 2023; Gros et al., 2017). Among these constituents, mineral surfaces such as Fe- and Al-(oxyhydr)oxides, calcium phosphates, silicates, and carbonates exhibit a strong affinity for binding phosphates (Bellier et al., 2006; Liu et al., 2012; Minamisawa et al., 2022; Okano et al., 2013; Tunesi et al., 1999). Notably, Fe- and Al-(oxyhydr)oxides play a pivotal role as the principal adsorbents of phosphates in soils (Borggaard, 2001; Borggaard et al., 2004; Elzinga and Sparks, 2007; Zhong et al., 2007). The high affinity of phosphates for these oxides stems from their ability to form stable covalent bonds with the surfaces of these oxides, termed inner-sphere surface complexes (Ahmed et al., 2019; Dimirkou et al., 2002; Kruse et al., 2015; Y. T. Wang et al., 2016). Among these oxyhydroxides, goethite (α-FeOOH) stands out as the most prevalent pedogenic reactive ferric iron Fe(III) mineral and plays a critical role for P fixation in soils (Arai and Sparks, 2007; Chitrakar et al., 2006; Cornell and Schwertmann, 2003; Tsao et al., 2011).

Considerable experimental and theoretical research endeavors have been directed toward exploring the mechanisms involved in the adsorption and binding of phosphates to oxyhydroxides and particularly the goethite surface. Examples of such studies include those by Ahmed et al. (2023), Amadou et al. (2022), Antelo et al. (2005), Arroyave et al. (2018, Boukemara et al. (2016), Luengo et al. (2006), and Y. T. Wang et al. (2016). These studies, along with others, aimed to clarify the impact of key factors such as the type, nature, and molecular configuration of both the phosphate and the adsorbent (Ognalaga et al., 1994; Ruttenberg and Sulak, 2011; Yan et al., 2014), P concentration (Arroyave et al., 2018; Luengo et al., 2006), characteristics of mineral surfaces including their planes (Ahmed et al., 2019), surface crystallinity and morphology (Gypser et al., 2018), specific surface area, point of zero charge of the adsorbent surface (Strauss et al., 1997a, 1997b), binding motifs (Ahmed et al., 2019; Arai and Sparks, 2001; Kubicki et al., 2012; Tejedor-Tejedor and Anderson, 1990), water and solution pH (Ahmed et al., 2020; Arroyave et al., 2018; Gao and Mucci, 2001; Geelhoed et al., 1998, 1997; Strauss et al., 1997a), presence of background electrolytes with their respective ionic strengths (Barrow et al., 1980; Geelhoed et al., 1998, 1997), redox potential (Shaheen et al., 2022), and the presence of other competitive inorganic (Gao and Mucci, 2001; Geelhoed et al., 1997; Hongshao and Stanforth, 2001) and/or organic (Geelhoed et al., 1998; Guppy et al., 2005; Kubicki and Ohno, 2020) anions on the process and strength of P binding.

Regarding the role of OM in P adsorption, organic acids demonstrate a strong affinity to adsorb onto Al- and Fe-hydroxide surfaces, influencing various physicochemical properties of reactive surfaces. These properties include specific surface area, reactive OH groups, surface charge, and electrostatic properties, consequently altering the interactions between phosphates and the adsorption sites (Gu et al., 1994; Kaiser and Guggenberger, 2003; Yan et al., 2016). Moreover,

sorption experiments, along with infrared (IR) and X-ray spectroscopy as well as Density Functional Theory (DFT) analyses, indicated that organic acids tend to form inner-sphere complexes under acidic conditions and outer-sphere complexes under basic conditions, highlighting the significant role of the hydrogen bonding interactions (Duckworth and Martin, 2001; Han et al., 2020). As a result, organic acids compete effectively with phosphates for adsorption onto the surface, leading to enhanced phosphate mobility and surface dissolution (Furrer and Stumm, 1986; Guppy et al., 2005; Han et al., 2020). Notably, Geelhoed et al. (1998) found that citrate adsorption decreased phosphate adsorption at the goethite surface at low pH. Moreover, Johnson and Loeppert (2006) found that organic acids effectively release adsorbed P from ferrihydrite, with the efficiency increasing in the order oxalate ~ malonate ~ succinate < tartrate < malate < citrate. Additionally, Antelo et al. (2007) and Fu et al. (2013) observed a significant decrease in P adsorption upon covering the goethite surface with humic acid (HA). Moreover, H. Wang et al. (2016) and Wang et al. (2015a, 2015b) reported that humic acids reduce the specific surface area and isoelectric point of iron oxides (goethite, hematite, and ferrihydrite), thereby significantly decreasing P adsorption. In contrast, Borggaard et al. (2005) reported a limited effect on P adsorption at aluminum oxide, ferrihydrite, and goethite upon covering the surfaces with soil-derived OM. In a recent long-term desorption study by Gypser et al. (2019), utilizing competitive inorganic and organic anions to release adsorbed P from Fe- and Al-hydroxides, it was found that P desorption increased in the order $CaCl_2$ < $CaSO_4$ < humic acid < citric acid. A further desorption study by Gypser et al. (2021) showed that goethite exhibited the highest desorption, followed by gibbsite and then ferrihydrite upon applying both organic and inorganic competitors. Furthermore, a joint experimental-theoretical approach by Kubicki and Ohno (2020) demonstrated that salicylate can replace adsorbed phosphate on the goethite surface.

Despite considerable efforts in the literature, the mechanism underlying the competition between phosphates and organic acids at reactive surfaces, particularly in soil environments, has not been fully understood, especially at the molecular level. This challenge is attributed to the limitations of current analytical techniques, coupled with the complex and heterogeneous nature of soil constituents (Dakora and Phillips, 2002; Han et al., 2020). Even for a specific mineral surface, variations in surface planes, crystallinity, morphology, saturation, and binding motifs further complicate the analysis (Ahmed et al., 2023). To address this gap and tackle this complexity, a joint approach involving sorption experiments and molecular dynamics (MD) simulations (Ahmed et al., 2023; Kubicki, 2016; Osman et al., 2023) is proposed offering a promising avenue for gaining deeper insights into the nature of the interaction between each P and OM species with the adsorbent surface. Therefore, the primary objective of the present study is to investigate the impact of OM on P adsorption and the competitive interactions between OM and P through a combined experimental-theoretical approach. This contribution delves into the adsorption behavior of three distinct phosphate molecules involving orthophosphate (OP), glycerolphosphate (GP), and inositolhexaphosphate (IHP) on the goethite surface under controlled conditions, including constant pH and ionic strength, with three different scenarios for each phosphate molecule. These scenarios include adsorption onto bare goethite, adsorption onto goethite covered with OM, and simultaneous co-adsorption of P and OM onto bare goethite. This investigation utilizes two common soil OM compounds, citric acid (CIT), and histidine (HIS) (Negassa et al., 2008; Werdin-Pfisterer et al., 2012; Westergaard Strobel et al., 1999), to elucidate the underlying mechanisms.

2. Materials and methods

2.1. Goethite preparation

Goethite was prepared according to (Dultz et al., 2018), where a 10 *M* NaOH solution was added to a 0.5 *M* $FeCl_3$ solution ($FeCl_3.6H_2O$, Merck AG) with stirring continuously to bring the pH to 12. The resulting material was aged for 120 h at 55 ºC to be converted to goethite. Then the suspension was subjected to pH adjustment to 6 by adding 0.1 *M* HCl and followed by centrifugation-washing cycles with distilled water until the electrical conductivity was lower than 10 µS cm^{-1}. The prepared goethite was freeze-dried and stored as a powder for further analysis and experiments. For details about the purity, crystallinity, particle size, and specific surface area of goethite, refer to our earlier investigation by Ganta et al. (2021).

2.2. Reagents

All studied OM (citric acid (CIT): $C_6H_8O_7$; L-histidine (HIS): $C_6H_9N_3O_2$) and P compounds (potassium dihydrogen phosphate (ortho-phosphate (OP)): KH_2PO_4, *α*-glycerol phosphate (GP): $C_3H_9O_6P$, and myo-inositol hexakisphosphate (IHP): $C_6H_{18}O_{24}P_6$) used in the experiments were of analytical grade chemicals and purchased from Carl Roth GmbH and Sigma-Aldrich, respectively. Working solutions were prepared fresh daily by adding accurate quantities of reagents to the water solution of 0.01 *M* $CaCl_2$ as a background electrolyte.

2.3. Adsorption experiments

The adsorption experiments were conducted using three distinct approaches: 1. Single-component adsorption: In this approach, we employed pure goethite as an adsorbent for OP, GP, and IHP (see Ganta et al. (2021), 2. Organic matter-exposed goethite adsorption: Here, we examined the adsorption of various P compounds (OP, GP, and IHP) on goethite surfaces that had been previously exposed to (covered with) organic matter (OM) substances; and 3. Co-adsorption of P and OM: In this approach, we investigated the simultaneous adsorption of both P and OM at the bare surfaces of goethite. Two abundant OM substances present in the soil, each characterized by carboxylic groups that compete for binding with phosphates on the goethite surface, were utilized: citric acid (CIT) and L-histidine (HIS). CIT, a common low-molecular-weight organic ligand primarily derived from plant root exudations or organic matter decomposition (Kpomblekou-A and Tabatabai, 2003), leverages its hydroxyl and carboxyl active groups to influence phosphorus availability through processes such as ligand exchange, chelation, and complexation reactions (Drouillon and Merckx, 2003). HIS, another OM substance, incorporates carboxylic and amino groups, offering the potential to competitively bind with phosphates on the goethite surface.

In the first set of adsorption experiments , we prepared a 250 m*M* P L^{-1} stock solution for each P reagent (OP, GP, and IHP) in a 0.01 M $CaCl_2$ solution. A 20 mg sample of goethite was placed in a 50 mL centrifuge tube and equilibrated with 40 mL of each of ten different initial P concentrations (ranging from 0 to 5 m*M* P L^{-1}, in particular, 0, 0.05, 0.1, 0.15, 0.2, 0.3, 0.5, 1, 2, 3, and 5 m*M* P L^{-1}), achieved by dilution of the P stock in a 0.01 M $CaCl_2$ solution with a pH value of 5. After a 24-hour equilibrium period at 25 ºC under end-over-end shaking at 20 rpm, samples were centrifuged at 4500g for 15 minutes. The P content in the filtered supernatant was quantified using inductively coupled plasma-optical emission spectroscopy (ICP-OES) at 214.914 nm wavelength.

In the second series of experiments, P adsorption isotherms were determined after the equilibrium adsorption of OM compounds to goethite. To ensure a similar magnitude of OM coverage for the

goethite surface, it was necessary to acquire the sorption coefficients of CIT and HIS. Like the P adsorption procedure, the same was repeated for CIT and HIS compounds as adsorbents. The only difference was that the addition of background electrolytes to OM suspensions was excluded. The C content in the supernatant was determined by a TOC analyzer (Dimatec Analysentechnik GmbH, 45141 Essen, Germany). Based on the OM adsorption data, the equivalent C concentrations of CIT and HIS were extrapolated to achieve the same coverage of 500 µmol C g^{-1} goethite. Subsequently, a two-stage adsorption process was conducted with (1) equilibrating 20 mg of goethite with 40 mL of CIT/HIS solution for 24 h, centrifugation, and decanting the supernatant and (2) following the same P adsorption procedure using OP, GP, and IHP solutions as described above.

In the last series, a competition experiment was carried out with the addition of CIT and HIS reagents (similar concentrations related to the adsorption rate of 500 µmol C g^{-1}) to the background electrolyte (0.01 *M* $CaCl_2$ solution) and adjusting the pH value to 5. The P adsorption procedure was then repeated as described previously. It is noteworthy that all series of adsorption experiments were performed in triplicate and data were presented as the means of three repeats.

2.4. Modeling of sorption isotherms

To investigate and describe the adsorption behaviors of P compounds on goethite in the absence or presence of OM substances, the sorption data were fitted to the Freundlich and Langmuir models as the most widely used analytical isotherms. The Freundlich model is a two-parameter equation that describes the relationship between the equilibrium concentration of adsorbed and free adsorbates onto heterogeneous surfaces based on an assumed uniform adsorption energy distribution. The model considers that sorption energy decreases exponentially with increasing saturation in the surface and can be expressed as:

$$Q_{ads} = K_f C_{eq}^{nf} \quad (1)$$

where Q_{ads} is the amount of adsorbate adsorbed per unit mass (or surface area) of adsorbent, C_{eq} is the adsorbate equilibrium concentration in solution, and K_f and n_f are the Freundlich unit capacity factor (sorption capacity) and non-linearity Freundlich exponent, respectively (Freundlich, 1907). In the present study, Q_{ads}, C_{eq}, and K_f are expressed in µmol m^{-2}, µmol L^{-1}, and mol^{1-nf} L^{nf} m^{-2}, respectively. Notice that the Freundlich model assumes that the adsorption enthalpy depends on the amount of adsorbate. In the limit of small Q_{ads} where the adsorption enthalpy should not depend on Q_{ads}, one could describe the isotherm by a Langmuir model as well. The Langmuir adsorption theory assumes that the adsorbate forms a monolayer on a homogenous adsorbent surface. The following equation expresses the Langmuir isotherm:

$$Q_{ads} = (Q_{max} K_l C_{eq} / (1 + K_l C_{eq}) \quad (2)$$

where Q_{max} is the maximum amount of the adsorbate required to form a monolayer by having a complete saturation of all binding sites (µmol m^{-2}), K_l is the Langmuir adsorption constant (L $µmol^{-1}$) that is related to the sorption energy (Langmuir, 1918). To determine the Freundlich and Langmuir constants, non-linear regression was carried out for both adsorption isotherm equations (1) and (2). Moreover, the standard error of the regression (SER) for all data sets was calculated. SER provides an absolute measure of the typical distance that data points deviate from the regression line. Therefore, SER offers a more reliable indication of the goodness-of-fit than R^2, especially when dealing with non-linear regression.

2.5. Molecular modeling and computational details

To model the binding/adsorption of phosphate at the goethite surface and investigate the influence of OM on this binding process at a molecular level, several molecular models were constructed. The overall molecular modeling approach employed in this study is illustrated in Fig. 1. Three different phosphates, namely OP (H_2PO_4), GP ($C_3H_8O_6P$), and IHP ($C_6H_{12}O_{24}P_6$), were considered to analyze the complexation reactions between each phosphate and the goethite surface in the presence of water (refer to Fig. 1). Each constructed phosphate-goethite-water complex model, exemplified in Fig. 1, comprises the following components: 1) the goethite surface, 2) a single adsorbed phosphate molecule on the surface, and 3) water molecules surrounding the phosphate-goethite complex. Moreover, two additional molecular models were designed to investigate the binding behavior and strength of OM with the goethite surface. Here, each model featured a single OM molecule, either CIT or HIS, instead of the phosphate molecule in the case of P-goethite-water models.

Furthermore, models were developed that incorporated a one-to-one ratio of P to OM at the goethite surface to investigate the competition between P and OM towards their interaction with the goethite surface. Specifically, for CIT, molecular models were created, including 1OP-1CIT-goethite, 1GP-1CIT-goethite, and 1IHP-1CIT-goethite. Similarly, analogous molecular models were established for HIS. For each 1P:1OM pair, two molecular models were considered. One model placed the 1P-1OM complex directly on the goethite surface, while the other positioned the 1P-1OM complex in the bulk solution, away from the goethite surface.

For each complex involving P-goethite, OM-goethite, and 1P:1OM-goethite, the chosen goethite surface is the 100 surface, recognized as one of the most prevalent surface planes in soil systems (Cornell and Schwertmann, 2003; Rakovan et al., 1999). This goethite surface plane is modeled by replicating the goethite unit cell (lattice constants a = 9.95, b = 3.01, and c = 4.62 Å) twice in the x-direction, twelve times in the y-direction, and eight times in the z-direction. This results in a supercell of dimensions x = 19.9, y = 36.12, and z = 36.96 Å, composed of 3072 atoms (768 Fe, 768 O, and 1536 H atoms). The initial configurations of the P-goethite, OM-goethite, and 1P:1OM-goethite complexes are designed so that the phosphates (OP/GP/IHP) and OM (CIT and HIS) molecules, as well as 1P-1OM complexes, are nearby and bound to the goethite surface except for the cases of 1P-1OM complexes in the bulk solution. This design is based on insights from previous simulation studies (Ahmed et al., 2018b, 2019, 2020; Ganta et al., 2020a, 2021). To account for the influence of water on the P-goethite, OM-goethite, and 1P:1OM-goethite complexes, each modeled complex is solvated by water with a density of ≈ 1 g cm^{-3}. The water molecules were added perpendicular to the studied surface plane, extending to a height of ≈ 130 Å in the x direction. This results in a final supercell with dimensions x = 150, y = 36.12, and z = 36.96 Å.

Due to the substantial size of the P-goethite, OM-goethite, and 1P:1OM-goethite complexes being modeled (each comprising approximately 20 thousand atoms, including water), employing ab initio methods for simulation is computationally impractical (Kubicki, 2016; Ozboyaci et al., 2016). Consequently, the investigation of these models was conducted through molecular dynamics (MD) simulations utilizing an atomistic representation via force-field molecular mechanics. Here, the goethite surface is represented using the CLAYFF force field (Cygan et al., 2004), while water is modeled using the single point charge (SPC) water model (Berendsen et al., 1987), and P (OP/GP/IHP) and OM (CIT and HIST) are represented with the CHARMM force field (Jo et al., 2008).

Both the CLAYFF and CHARMM force fields are compatible with the SPC water model. The simulations are conducted under periodic boundary conditions in all three dimensions.

For each molecular model, an energy minimization was carried out, followed by a two-step canonical (NVT, i.e., constant number of atoms N, volume V, and temperature T) MD simulation, consisting of approximately 5 ns for equilibration and 20 ns for the production trajectory that were utilized for MD analysis. The time step was set to 2 fs, and a straight cutoff of 12 Å was employed in conjunction with the Verlet neighbor list scheme. Temperature control was achieved using the velocity-rescaling thermostat with a coupling constant of 0.1 ps, maintaining the temperature at 300K (Bussi et al., 2007). The interaction energy between every two subsystems of the P-goethite, OM-goethite, and 1P:1OM-goethite complexes in the presence of water was calculated along the production trajectory based on electrostatic Coulomb and van der Waals interactions. All calculations and corresponding analyses were conducted using the GROMACS program package, version 2019.4 (Abraham et al., 2015; Van Der Spoel et al., 2005).

To mimic the experimental pH condition (pH 5), the molecular models of P and OM were configured based on the most prevalent species for each molecular structure. Specifically, OP was represented as H_2PO4^-, GP as GP^-, IHP as IHP^{6-}, CIT as CIT^{2-}, and HIS as HIS^-. Additionally, all simulation boxes were neutralized with sodium ions (Na^+).

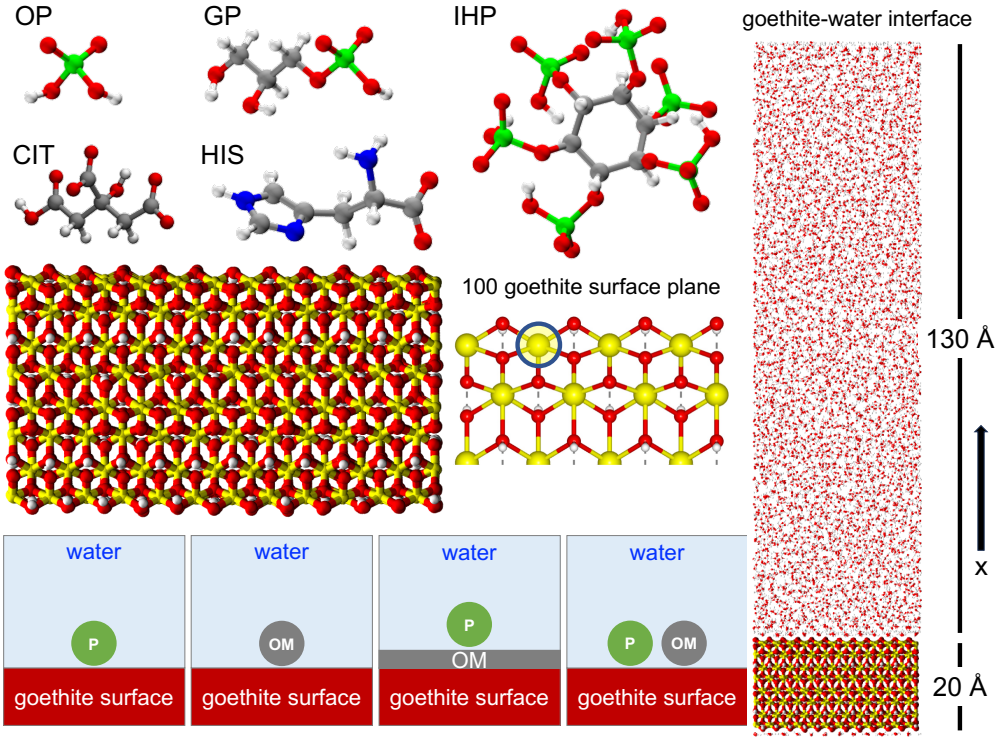

Figure 1. Illustration of the molecular modeling approach examining the impact of organic matter (OM) on the binding of phosphorus (P) at the interface between goethite and water. It includes representations of the chemical and three-dimensional structures of modeled P compounds (OP, GP, and IHP) and OM compounds (CIT and HIS). The figure also presents two side views of the modeled 100-goethite surface plane, with one providing a comprehensive view and the other zooming in on the coordination number of surface Fe atoms, highlighted within a circle (dashed lines denote hydrogen bonds). Additionally, schematic representations of four adsorption scenarios are provided: P adsorption at the goethite surface, OM adsorption at the goethite surface, P adsorption at the goethite surface previously covered with OM, and simultaneous co-adsorption of P and OM at the goethite surface. Furthermore, the figure displays a representative example depicting the goethite-water interface. Different atoms are depicted in varying colors: H, C, N, O, P, and Fe atoms are visualized in white, red, gray, blue, green, and yellow, respectively.

3. Results and discussion

3.1. Experimental results

3.1.1. General overview

The results of the adsorption experiments provide valuable insights into the interactions between phosphates and the goethite surface. Specifically, the P adsorption (per mol P) exhibits a consistent order of GP < OP < IHP across all experimental conditions, indicating a systematic variation in adsorption capacity (see Fig. 2 and Fig. S1 in the supporting information). This pattern highlights IHP consistently having the highest adsorption capacity, while GP consistently shows the lowest values. Importantly, this trend consistently holds across all treatments employed in the present adsorption experiments, whether involving organic matter (OM), acetic acid (CIT), or histidine (HIS), or not, and irrespective of the specific treatment approach, including covering the surface with OM and simultaneous co-adsorption. This order remains stable despite variations in individual adsorption capacities, indicating a robust trend beyond the specific experimental conditions employed in this study.

The adsorption data presented here were subjected to fitting with various adsorption isotherm models. Among these models, Langmuir and Freundlich exhibited superior fitting performance, as evidenced by SER values. Notably, the Freundlich model consistently outperformed the Langmuir model in all adsorption experiments, demonstrating lower SER values, except for the GP adsorption on the goethite surface covered with CIT, as indicated in Table 1. A comprehensive discussion follows, incorporating precise numerical comparisons, focusing on the relevant Freundlich and Langmuir fitted parameters in the context of OP, GP, and IHP adsorption under various treatments. This discussion will be organized as follows: initially examining the impact of each goethite treatment on the variations in adsorption among OP, GP, and IHP, and subsequently, analyzing how the different treatments influence the adsorption of each P molecular system (OP, GP, and IHP).

In the context of the Langmuir isotherm, the parameter Q_{max}, representing the maximum adsorption capacity, plays a pivotal role in assessing the adsorption strength and the surface's affinity. It signifies the quantity of adsorbate required to occupy all active binding sites and establish a complete monolayer saturation. The Q_{max} values exhibit an ascending order of GP < OP < IHP across all experimental conditions. In the absence of OM, IHP consistently exhibits markedly higher adsorption capacity than both OP and GP, see Table 1, Fig. 2, and Figs. S1-S2 in the supporting information. Specifically, IHP's adsorption capacity is approximately 1.3 times that of OP and nearly 8.5 times that of GP. The sequence of adsorption (GP < OP < IHP) is consistent with the observations made by Amadou et al. (2022) for the adsorption of the same phosphates on the goethite surface. Similarly, Yan et al. (2014) noted a similar trend, with GP exhibiting the least affinity and IHP demonstrating the highest affinity when adsorbed on amorphous $Al(OH)_3$ surfaces. However, this trend was reversed when the same phosphates were adsorbed onto the gibbsite (Amadou et al., 2022) and the boehmite (Yan et al., 2014). Further, Yan et al. (2014) found that on α-Al_2O_3 surfaces, IHP had the least affinity, OP had the highest, and GP fell in between. These findings highlight the influence of both phosphate molecular structure and mineral surface type and crystallinity on the adsorption process. In this context, Yan et al. (2014) indicated that the mass-based phosphorus adsorption capacities increase with decreasing mineral crystallinity, following the sequence of α-Al_2O_3 < boehmite < amorphous $Al(OH)_3$.

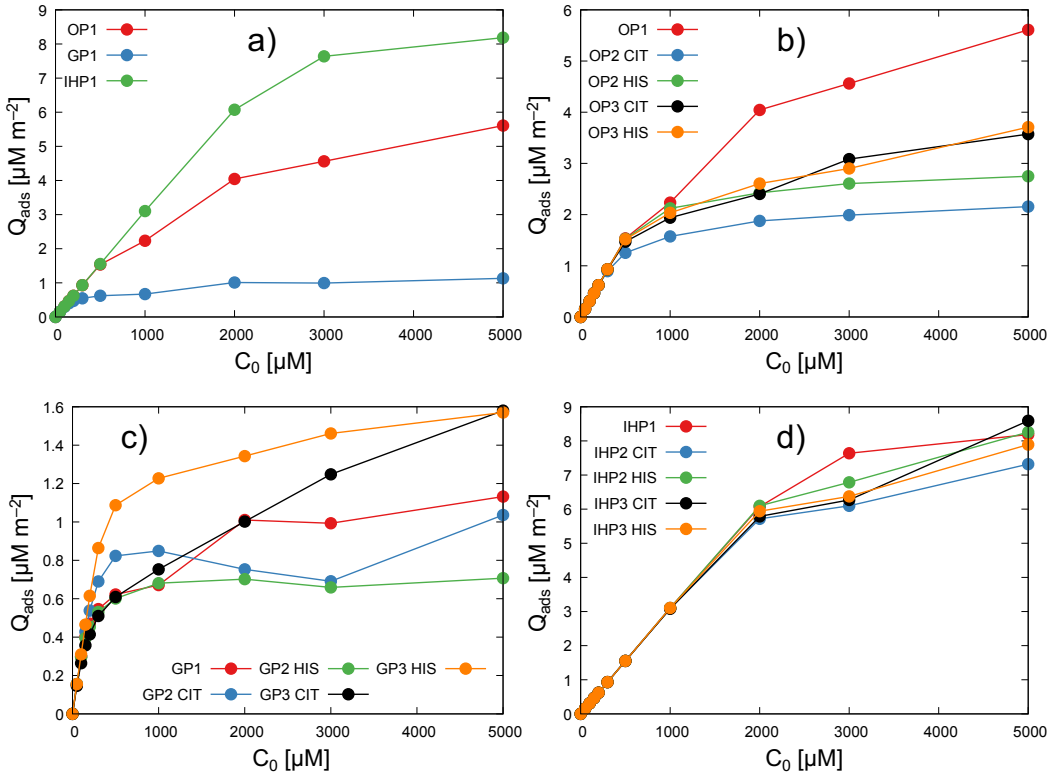

Figure 2. The relationship between P adsorption per unit surface area (Q_{ads}, µmol m^{-2}) and the corresponding initial P concentration (C_0, µmol L^{-1}) for orthophosphate (OP), glycerolphosphate (GP), and inositolhexaphosphate (IHP) under various experimental conditions. Panel (a) illustrates OP, GP, and IHP adsorption on the bare goethite surface, while panels (b), (c), and (d) showcase P adsorption at the goethite surface with different experimental conditions for OP, GP, and IHP, respectively. The numerical symbols 1, 2, and 3 represent P adsorption on bare goethite, goethite covered with organic matter (OM), and P plus OM co-adsorption, respectively. This notation applies to OP, GP, and IHP. CIT and HIS denote adsorption in the presence of citric acid or histidine, respectively, whether through covering the surface coverage with OM or co-adsorption. Lines connect data points for clarity.

3.1.2. Impact of OM treatments on P adsorption behavior

When covering the goethite surface with CIT, IHP's adsorption capacity is roughly 3.5 times that of OP and approximately 7.8 times that of GP. In the case of HIS, IHP's adsorption capacity is approximately 3.1 times that of OP and nearly 11.5 times that of GP. These findings emphasize a more pronounced influence of organic coatings on diminishing P adsorption capacities, particularly for GP in the presence of HIS and for OP in the presence of CIT. In simultaneous co-adsorption scenarios with CIT, IHP's maximum adsorption capacity is approximately 2.5 times that of OP and around 5.1 times that of GP. Similarly, with HIS, IHP's maximum adsorption capacity is approximately 2.5 times also that of OP and nearly 5.5 times that of GP. In conclusion, these comparisons relevant to the maximum adsorption capacity reveal no significant difference between CIT and HIS in simultaneous co-adsorption scenarios. However, a noteworthy reduction is observed in the case of OM coatings compared to the simultaneous co-adsorption of phosphates and OM.

Regarding the Freundlich isotherm, the combination of both the Freundlich unit capacity (K_f) and exponent (n_f) is crucial in assessing adsorption strength. Higher values for both K_f and the exponent n_f are indicative of more robust adsorption and elevated capacities. This holds for the exponent n_f, especially in scenarios where the equilibrium concentration (C_{eq}) is higher than 1. It should be noted that a minor alteration in the exponent tends to have a more pronounced impact on adsorption

strength than changes in K_f alone. Thus, caution is advised when interpreting the fitted Freundlich isotherm parameters, emphasizing the need to consider both K_f and, particularly, n_f, especially when n_f varies significantly for data from different adsorption experiments. In the present study, K_f values exhibit an ascending order of GP < OP < IHP across all experimental conditions. This sequence implies that in the context of goethite surface adsorption, IHP demonstrates the most robust adsorption and possesses the highest capacity, followed by OP and GP. This comes in accord with the conclusion obtained by the Langmuir Q_{max} values. As for the Freundlich exponent (n_f), it is crucial to underscore that this exponent can offer insights not only into the adsorption strength but also into the adsorption mechanism. Specifically, n_f values below 1, observed in all present adsorption experiments, indicate that the sorption mechanism is primarily dominated by adsorption rather than absorption (Ahmed et al., 2015, 2014). Moreover, n_f values below 1 imply that as the P concentration/loading increases, the binding energy between P compounds and the surfaces diminishes. In other words, for lower n_f values, the affinity of the goethite surface to adsorb/bind a P molecule decreases as the P concentration/loading rises. The validation and clarification of understanding and interpretation of both K_f and n_f in this manner are demonstrated in Fig. S3 in the supporting information. A detailed interpretation of the various treatments is provided in the subsequent discussion.

In the context of P adsorption on bare goethite (i.e., in the absence of OM), the sequence of n_f values (IHP (0.074) < GP (0.199) < OP (0.259), see Table 1) implies a reduction in binding energy with an increase in P loading, following the order OP < GP < IHP. This signifies that the bare goethite surface exhibits an escalating affinity to adsorb/bind a P molecule in the order IHP < GP < OP as the P concentration rises. Despite IHP displaying the most robust adsorption, the untreated goethite surface has the highest affinity to bind OP at higher P concentrations. This observation may be attributed to the bulky size of IHP, which occupies and blocks more active sites and experiences self-repulsion within IHP molecules compared to OP.

For goethite covered with CIT, the n_f values sequence (GP (0.112) < IHP (0.120) < OP (0.150)) suggests that the affinity of the CIT-covered surface to adsorb/bind a P molecule increases with P concentration in the order GP < IHP < OP. Similar to the case of bare goethite, the CIT-covered surface exhibits the highest binding affinity for OP, but the lowest for GP at high P concentrations. This is indicative not only of the surface interaction but also of relatively stronger interactions between CIT and OP compared to GP. In the scenario of goethite covered with HIS, the n_f values sequence (IHP (0.068) < OP (0.100) < GP (0.110)) suggests that the affinity of the HIS-covered surface to adsorb/bind a P molecule increases with P concentration, following the order IHP < OP < GP. This implies that, at higher P concentrations, the HIS-covered surface exhibits a preference for GP binding, highlighting relatively stronger interactions between HIS and GP. This could substantiate the conclusion on the enhanced adsorption of GP on goethite in the case of co-adsorption with organic matter, specifically HIS.

In the context of co-adsorption of P with CIT on the goethite surface, the sequence of n_f values (IHP (0.160) < OP (0.181) < GP (0.327)) implies that the surface's affinity to adsorb/bind a P molecule rises with increasing P concentration, following the order IHP < OP < GP. This suggests that, at higher P concentrations, the surface demonstrates a preference for GP binding, emphasizing favorable interactions and complexation between CIT and GP at high GP concentrations. Similarly, in the context of co-adsorption, but with HIS instead of CIT, the sequence of n_f values (IHP (0.080)

< GP (0.113) < OP (0.171)) indicates that the surface's affinity to adsorb/bind a P molecule increases with P concentration in the order IHP < GP < OP. This implies that, at higher P concentrations, the surface exhibits a preference for binding OP followed by GP, highlighting favorable interactions and complexation of HIS with OP and GP at high P concentrations.

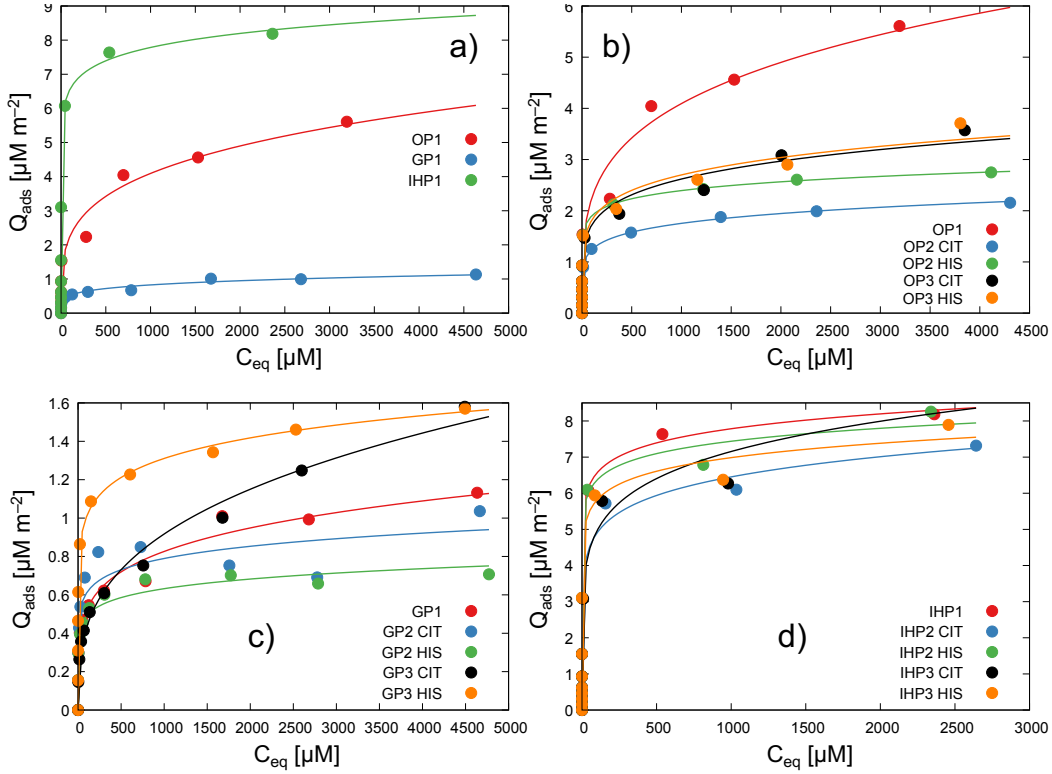

Figure 3. The relationship between P adsorption per unit surface area (Q_{ads}, µmol m^{-2}) and the corresponding equilibrium P concentration (C_{eq}, µmol L^{-1}) in solution for OP, GP, and IHP under various experimental conditions fitted according to Freundlich isotherm. Panel (a) shows OP, GP, and IHP adsorption on the bare goethite surface, while panels (b), (c), and (d) showcase P adsorption at the goethite surface with different experimental conditions for OP, GP, and IHP, respectively. The numerical symbols 1, 2, and 3 represent P adsorption on bare goethite, goethite covered with organic matter (OM), and P plus OM co-adsorption, respectively. These annotations apply to OP, GP, and IHP. CIT and HIS denote adsorption in the presence of citric acid or histidine, respectively, whether through covering the surface coverage with OM or co-adsorption.

3.1.3. Impact of OM on OP adsorption

Let us discuss the adsorption patterns of OP on the goethite surface under two distinct scenarios: firstly, examining the impact of OM on OP adsorption when goethite is covered/coated with OM, and secondly, considering the simultaneous co-adsorption of OP and OM on goethite. Notably, when the goethite surface was covered with CIT, a pronounced decrease in OP adsorption was evident compared to the OP adsorption at bare goethite (see Fig. 3b). The maximum adsorption capacity decreased from 6.25 to 1.85 µmol m^{-2} (see Table 1), representing a reduction by factor 3.4. This translates to a 70% decrease in the maximum adsorption capacity of OP to goethite when the surface is covered with CIT. This underscores the inhibitory impact of CIT on OP adsorption, likely attributed to CIT molecules occupying binding sites on the goethite surface, consequently restricting the availability of sites for OP adsorption. Likewise, the application of HIS to the goethite surface led also to a notable decrease in OP adsorption. In this instance, the maximum adsorption capacity decreased from 6.25 to 2.49 µmol m^{-2}, representing a reduction by factor 2.5 (~ 60% decrease).

Analogous to CIT, this decrease can be attributed to the strong adsorption affinity of HIS for the goethite surface, effectively competing with OP for the available binding sites and consequently diminishing OP adsorption.

The highlighted stronger inhibitory influence of CIT on OP adsorption is attributed to its higher affinity for surface sites. This is linked to the presence of more reactive functional groups in CIT compared to HIS. CIT possesses three carboxylate functional groups and one hydroxyl group, all of which are active and capable of binding to the goethite surface through ligand exchange and/or complexation reactions. In contrast, HIS contains one carboxylate and one amino group, providing it with the potential to bind to the goethite surface. Furthermore, under the current experimental conditions (pH 5), the increased negative charge of CIT (-2 for citrate) compared to HIS (-1) is notable for its involvement in binding to the positively charged active sites on the goethite surface through electrostatic interactions. This indicates that the nature of OM plays a crucial role in determining the degree of inhibition in P adsorption, with the presence of reactive and charged functional groups being a key determining factor.

The present results and their interpretation are consistent with those of Antelo et al. (2007), who noted a significant decrease in P adsorption when the goethite surface was coated with soil-derived humic acid (HA). Moreover, studies conducted by Dultz et al. (2018) and Kaiser and Guggenberger (2003) demonstrated that OM rich in acidic functional groups promotes aggregation with goethite, influencing specific surface area and micropore clogging. H. Wang et al. (2016) and Wang et al. (2015a) confirmed that the addition of humic acid reduces the specific surface area and isoelectric point of iron oxides, thereby affecting P adsorption. Furthermore, Fu et al. (2013) used Fourier transform infrared spectrometry (FTIR) to reveal fewer hydroxyl groups on goethite after soil-derived HA adsorption, resulting in inhibited adsorption and weaker P affinity. Their investigation illustrated that coating the goethite surface with HA can significantly reduce OP adsorption by as much as 27.8%. Several other studies, including those of H. Wang et al. (2016), Wang et al. (2015a), and Weng et al. (2008) highlighted that adsorbed HA on iron oxides leads to a reduction in P adsorption. In contrast, Borggaard et al. (2005) reported a limited effect on P adsorption at aluminum oxide, ferrihydrite, and goethite upon covering the surfaces with soil-derived OM.

The simultaneous co-adsorption of OM and OP on the goethite surface led to a decrease in OP adsorption compared to the adsorption on bare goethite. This reduction was nearly identical for both CIT and HIS, with the maximum adsorption capacity decreasing by factor 2.2 (~ 54% decrease) compared to the bare goethite case. This suggests similar competitive effects of both CIT and HIS when present simultaneously in the solution with OP. This may also imply comparable complexation reactions in the solution between CIT and OP, as well as HIS and OP. Furthermore, under both CIT and HIS treatments, OP exhibited a more significant reduction in adsorption when the goethite surface was covered with OM compared to the scenario where OP was co-adsorbed simultaneously with OM. This reduction can be attributed to the fact that in the covering scenario, OM (CIT and HIS) already bound to the goethite surface block most of the active binding sites, impeding OP adsorption to a greater extent compared to the competition between OM and OP in the co-adsorption scenario. Notably, this behavior is more pronounced in the case of CIT than HIS, indicating the greater affinity of CIT to undergo stronger adsorption at the goethite surface and block more active sites than the HIS case. Eventually, this emphasizes the substantial influence of surface modification, wherein the presence of OM, whether as a coating on the goethite surface or co-adsorbed with OP, plays a pivotal

role in reducing OP adsorption. This highlights the significance of taking surface modifications into account when studying the behavior of P compounds in environmental systems.

The observed decrease in P adsorption, particularly concerning the co-adsorption of OM and OP, aligns with the findings of previous studies conducted by Sibanda and Young (1986), Antelo et al. (2007), and Fu et al. (2013). These studies suggested that OM derived from soil exhibited a competitive interaction with phosphate, leading to the inhibition of OP adsorption by goethite. For example, Sibanda and Young (1986) investigated the competitive effect of humic acid (HA) and fulvic acid (FA) on P adsorption on goethite, gibbsite, and two tropical soils at pH values of 4 and 7. They observed reductions in P adsorption when applying HA and FA across all cases, with this effect being more pronounced for P adsorption on goethite and gibbsite in the presence of HA at a lower pH (pH 4). Further, Antelo et al. (2007) studied the competitive impact of HA on phosphate adsorption onto goethite across varying pH and ionic strength conditions. Their findings revealed a significant influence of HA presence on P adsorption, with a more pronounced effect observed at lower pH levels compared to higher pH levels. This was attributed to the greater adsorption capacity of HA at the goethite surface under acidic conditions. At pH 4.5, HA could reduce P adsorption by as much as 45%, while at pH 7.0, the reduction was up to 25%. They also observed a relatively higher reduction in P adsorption when the goethite surface had previously adsorbed HA, in contrast to the simultaneous adsorption of P and HA. This aligns with our current observation regarding the stronger impact of covering the surface with OM on P (particularly OP) adsorption compared to the concurrent co-adsorption of P and OM. Moreover, Fu et al. (2013) explored a notable decrease in P adsorption when co-adsorbed with soil-derived HA. Similar to our findings, Antelo et al. (2007) also noted a larger reduction in P adsorption when the surface was pre-covered with HA compared to the simultaneous co-adsorption scenario. In contrast, Borggaard et al. (2005) reported small reductions in P adsorption at goethite by 4 to 11.2 % in the presence of HA in a co-adsorption scenario. These small effects can be explained by the proportions of molecular structures in HA that are not involved in interactions with goethite surfaces, and by P-binding metals like Al and Fe that can be incorporated in the HA (e.g., see Leinweber and Schulten (1999)).

3.1.4. Impact of OM on GP adsorption

For GP, the adsorption behavior at the goethite surface is complex and influenced by several factors, including initial P concentrations, adsorption conditions or treatment type (coverage versus co-adsorption), and the type of OM (CIT versus HIS). Key observations reveal essential insights into this complexity. Generally, co-adsorption with OM (CIT or HIS) on the goethite surface enhanced GP adsorption compared to the bare goethite surface. The maximum adsorption capacity increased from 0.95 µmol m^{-2} for bare goethite to 1.40 and 1.31 µmol m^{-2} for co-adsorption with CIT and HIS, respectively, representing increases of 1.5 and 1.4 times for CIT and HIS cases. This corresponds to enhancements of 47% and 38% in the maximum adsorption of GP when co-adsorbed with CIT and HIS, respectively. This enhancement may be attributed to the potential formation of stable complexes between GP and OM (CIT and HIS), wherein these complexes exhibit a higher tendency to bind and adsorb onto the goethite surface compared to the individual GP scenario. A possible mechanism for this adsorption could be via OM (CIT and HIS) serving as bridges between the goethite surface and GP, thereby facilitating GP binding and the subsequent adsorption process. A comparison between CIT and HIS in the co-adsorption process with GP indicates higher and more

favorable adsorption for GP in the presence of HIS at an initial GP concentration of up to 3 mM, suggesting a more favorable interaction/complexation for GP with HIS than with CIT. This is supported by the higher Freundlich unit capacity K_f in the HIS case (0.599) in comparison to the CIT scenario (0.096), see Table 1. However, a further increase in the initial concentration reverses this observation, enhancing GP adsorption in the presence of CIT compared to HIS and leading to a higher maximum adsorption capacity for CIT (1.40 µmol m^{-2}) compared to HIS (1.31 µmol m^{-2}) at high GP concentrations. This could be explained by the higher affinity of CIT for the goethite surface compared to HIS as observed for the OP case, thus stabilizing more GP molecules in the presence of CIT, especially at high GP concentrations. This is bolstered by the higher Freundlich exponent n_f in the CIT case (0.327) compared to the HIS scenario (0.113), as shown in Table 1. This points to a higher affinity of the surface to adsorb more GP molecules in the CIT case than in the HIS case, with an increase in P concentration.

Covering the goethite surface with OM (CIT or HIS) resulted in an overall decrease in GP adsorption compared to that on the bare goethite surface. This reduction can be attributed to the occupation of binding sites on the goethite surface by OM, limiting the availability of sites for GP adsorption. In general, the maximum adsorption capacity decreased from 0.95 µmol m^{-2} for bare goethite to 0.83 and 0.66 µmol m^{-2} for CIT and HIS-covered surfaces, respectively. This corresponds to a reduction by factors 1.15 and 1.44 for the CIT and HIS cases, representing reductions of approximately 13% and 31%, respectively. This highlights the inhibitory effect of OM, particularly HIS when the surface is pre-covered with OM before GP adsorption. A detailed examination of GP adsorption on the goethite surface covered with OM reveals a two-step adsorption process based on the initial concentration. At initial GP concentrations up to 1 mM, GP exhibits higher and more favorable adsorption in the presence of OM compared to GP adsorption on bare goethite. This suggests a favorable complexation for GP with OM, particularly CIT, enhancing GP adsorption. This is supported by an increase in the Freundlich unit capacity (K_f) for GP adsorption in the order of bare goethite (0.208) < goethite covered with HIS (0.295) < goethite covered with CIT (0.365), as indicated in Table 1. However, at initial concentrations exceeding 1 mM, this trend reverses, resulting in reduced GP adsorption in the presence of CIT and HIS, leading to lower maximum adsorption capacities at higher GP concentrations compared to the bare goethite case. This is supported by the lower Freundlich exponent (n_f) in the presence of CIT (0.112) and HIS (0.110) compared to the bare goethite scenario (0.199), as shown in Table 1. This reduction can be attributed to the increased blocking of active binding sites at the goethite surface at higher GP concentrations.

3.1.5. Impact of OM on IHP adsorption

In the case of IHP adsorption onto goethite surfaces, the impact of OM is notably less substantial compared to OP and GP. At low initial P concentrations, up to 2 mM, Fig. 2d depicts an insignificant alteration in IHP adsorption when covering the goethite surface with OM and simultaneous co-adsorption, either with CIT or HIS. Despite the observed reduction in IHP adsorption, especially at higher initial IHP concentrations (see Fig. 2d), this decrease is relatively small for both scenarios. For the goethite surface covered with CIT and HIS, it becomes evident that IHP exhibits lower adsorption when goethite is coated with CIT, particularly at elevated initial P concentrations (see Fig. 2d). This highlights the inhibitory effect of OM, particularly CIT when the surface is pre-covered with OM before IHP adsorption. This is evident in the maximum IHP adsorption capacity, which decreased

from 8.05 μmol m^{-2} in the case of bare goethite to 6.47 and 7.59 μmol m^{-2} for CIT and HIS cases, respectively. This represents a reduction of 1.24 and 1.06 times for the CIT and HIS cases, corresponding to reductions of approximately 20% and 6%, respectively. For the IHP co-adsorption with individual CIT and HIS on the goethite surface, there is negligible difference between both cases. They resulted in maximum adsorption capacities of 7.16 and 7.27 μmol m^{-2} for co-adsorption with CIT and HIS, respectively. This corresponds to reductions of 11% and 10% in the maximum adsorption capacity for the CIT and HIS cases, respectively. Comparing the co-adsorption and covering the surface scenarios for HIS, a slighter reduction in the IHP maximum adsorption capacity (4%) is observed in the case of co-adsorption. In contrast, a slightly lower reduction in the IHP maximum adsorption capacity (9%) is observed in the case of goethite covered with CIT rather than undergoing simultaneous co-adsorption. Eventually, these findings highlight the limited impact of OM on altering the adsorption of IHP on goethite surfaces, especially at lower P concentrations. Nevertheless, at higher P concentrations, there are subtle variations in adsorption behavior depending on the type and application scenarios of OM, although these variations are relatively minor.

Table 1. Freundlich and Langmuir isotherms coefficients of adsorption of phosphates (OP, GP, and IHP) at goethite at different experimental conditions: adsorption of phosphates at pure goethite (P@G), adsorption of phosphates at covered goethite with organic matter (OM, P@CIT-G, and P@HIS-G), and simultaneous co-adsorption of phosphates and organic matter at goethite (P+CIT@G and P+HIS@G). OM here are citric acid (CIT) and L-histidine (HIS). K_f, K_l, and Q_{max} are expressed in $mol^{1-nf}\ L^{nf}\ m^{-2}$, L μmol^{-1}, and $\mu mol\ m^{-2}$, respectively.

Treatments	**OP**						**GP**						**IHP**					
	Freundlich			Langmuir			Freundlich			Langmuir			Freundlich			Langmuir		
	K_f	n_f	*SER*	Q_{max}	K_l	*SER*	K_f	n_f	*SER*	Q_{max}	K_l	*SER*	K_f	n_f	*SER*	Q_{max}	K_l	*SER*
P@G	0.685	0.259	0.521	6.252	0.002	0.660	0.208	0.199	0.074	0.949	0.018	0.164	4.660	0.074	1.233	8.049	0.070	1.234
P@CIT-G	0.624	0.150	0.194	1.851	0.076	0.310	0.365	0.112	0.123	0.831	0.093	0.108	2.822	0.120	0.708	6.471	0.209	0.758
P@HIS-G	1.202	0.100	0.284	2.487	0.202	0.434	0.295	0.110	0.067	0.658	0.078	0.079	4.654	0.068	1.252	7.593	0.113	1.275
P+CIT@G	0.751	0.181	0.335	2.861	0.035	0.551	0.096	0.327	0.055	1.399	0.003	0.185	2.376	0.160	0.770	7.162	0.088	0.915
P+HIS@G	0.829	0.171	0.455	2.863	0.093	0.571	0.599	0.113	0.194	1.308	0.324	0.253	4.020	0.080	1.254	7.270	0.049	1.276

3.2. Simulation results

To validate our interpretations of the present experimental outcomes, MD simulations were conducted to address key questions: Does the order of P binding/adsorption at the goethite surface follow as GP < OP < IHP? Does organic matter (OM) exhibit significant binding to the goethite surface, leading to competition with P and consequent reduction in P binding? Does CIT bind more strongly to the goethite surface than HIS? What about the binding nature particularly for OM (electrostatic versus van der Waals interactions)? Does OM produce an unfavorable electrostatic field around the adsorbed OM molecule/molecules preventing/ limiting the P adsorption? If OM competes with P and diminishes binding, how does OM (CIT and HIS) enhance GP adsorption in the co-adsorption scenario? Which exerts a stronger binding effect, IHP or OM? If IHP exhibits stronger binding, how does OM reduce IHP binding?

The present molecular modeling approach is focused on characterizing the relatively large model size of the P/OM-goethite-water complexes through MD simulations employing force-field-based molecular mechanics. Consequently, the current study will revolve around discussing the processes of P binding and the impact of OM, without delving into the intricacies of bond formation and dissociation. These aspects, extensively discussed in our previous studies, entailed a comprehensive understanding of the P-binding mechanism to soil constituents at the quantum mechanics level (Ahmed et al., 2023, 2020, 2019, 2018b; Ganta et al., 2021, 2020a, 2020b, 2019; Shaheen et al., 2022). Those studies aimed to elucidate the effects of various key factors on the P-binding process and its strength. These factors include the type and nature of P-containing compounds, the molecular configuration of both the phosphate and the adsorbent, characteristics of mineral surfaces including their planes, and morphology, binding motifs, water and solution pH, and redox potential. For example, phosphates like OP and GP with single phosphate groups form stable monodentate (**M**) and bidentate (**B**) binding motifs. On the other hand, phosphates containing multiple phosphate groups like IHP can bind to mineral surfaces through more than one phosphate group, forming various stable motifs like **M**, 2 **M**, and 3 **M**. The interaction energies of phosphates and water with goethite and diaspore surfaces increase in the order water < GP < OP < IHP (Ganta et al., 2021, 2020a), indicating that phosphates could displace water molecules at these surfaces, with IHP potentially replacing OP and GP. Additionally, water plays a critical role in controlling phosphate binding through hydrogen bond formation, dissociation at the surface, proton transfer processes, and covalent/coordination bond formation with the surface. Intramolecular hydrogen bonds between adjacent phosphate groups in IHP can induce strain into IHP-mineral complexes, affecting motif stability and leading to the dissociation of certain covalent bonds and instability of specific motifs.

3.2.1. Characterization of the goethite-water interface

To comprehend the binding mechanism of P and OM at the goethite surface, as well as their competitive interactions, our initial focus will be on characterizing the goethite-water interface. Figure 4 illustrates the distribution of charge density of a goethite-water molecular model along the x-axis of the simulation box, perpendicular to the goethite-water interface. It is important

to note that the charge distribution is integrated over the other axes (y and z). In this representation, intense peaks with positive charges depicted in red correspond to Fe atoms of the goethite, while smaller peaks are attributed to H atoms of the goethite surface. Conversely, intense negative peaks depicted in red correspond to O atoms of the goethite surface. Among these peaks, the relatively smaller ones proximate to the H-peaks represent hydroxide ions (OH^-) of the goethite, whereas the relatively larger ones, farther from the H-peaks, correspond to non-protonated oxygen atoms of the goethite, i.e., O^{2-}. Observing the surface reveals termination with negatively charged OH^- (peak around 20.5 Å for O atoms), followed in the direction of the goethite bulk by two subsequent positively charged peaks around 20.1 Å (for H atoms) and 19.7 Å (for Fe atoms). This suggests the presence of a positively active site at the goethite surface capable of binding and adsorbing anions such as phosphates and carboxylates, despite the negatively charged O atoms at the surface top. Due to the surface termination with a negative charge, certain water molecules engage with the surface by aligning themselves with H atoms (positively charged) facing the surface within the Helmholtz layer, which generates the initial small positively charged peak around 21.3 Å, illustrated in blue in Fig. 4. Subsequently, the majority of water molecules near the surface reorient so that O atoms face the surface while H atoms face towards the bulk of the water. This leads to the emergence of the primary and largest negatively charged peak of water (O atoms) at the interface around 21.7 Å, succeeded by the largest positively charged peak of water (H atoms) around 22.4 Å. For further elaboration and clarification, this distribution of charge density along the goethite-water interface including the Helmholtz layer and the interpretation of peaks corresponding to Fe^{3+}, O^{2-}, and OH^- of goethite, and $O^{\delta-}$ and $H^{\delta+}$ of water are illustrated in Fig. S4 in the supporting information. The strong electrostatic interaction between water and the surface at the interface, coupled with the presence of active sites at the surface, leads to a high density of water at the surface, decreasing in the direction of the water bulk, thus conforming to the normal distribution and density of liquid water (refer to Figs. 4b, 4d-f). For example, in Fig. 4e-f, water exhibits significantly high mass density near the surface, with the first layer reaching approximately four times the normal density of liquid water (about 4000 kg m^{-3}). The density decreases to around twice the normal density (2000 kg m^{-3}) in the second layer. Moving away from the surface, water density gradually decreases, reaching normal liquid density at approximately 10 Å from the surface.

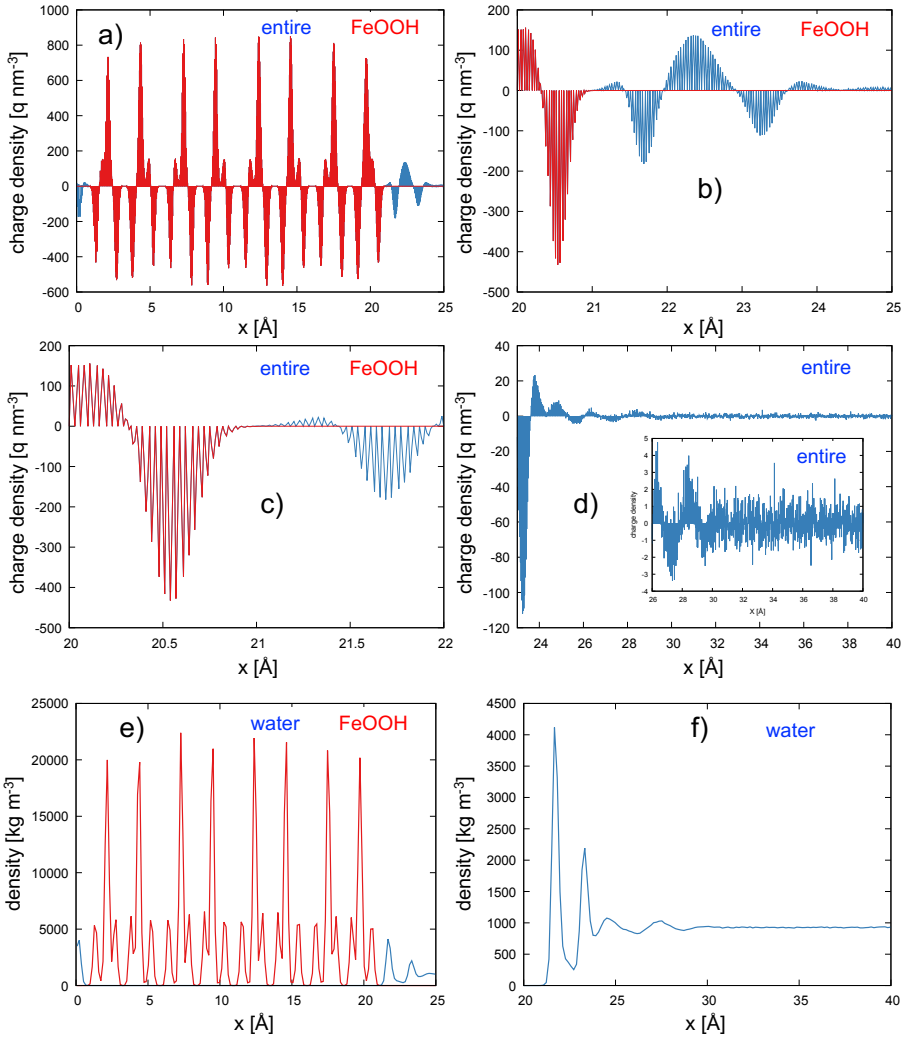

Figure 4. Visualization of the distribution of charge density (a-d) along the axis perpendicular (x) to the interface for both the goethite surface (red) and the entire system (blue) at various distances within the simulation box. The simulation box spans from x = 0 to x = 150 Å, with goethite primarily positioned around x = 0-20 Å during the MD simulation. In addition, the mass density (e-f) along various distances in the simulation box is presented.

The electric potential of the goethite-water system described above exhibits positive values along the x-axis, with peaks representing maximum positive charge densities observed at the positions of Fe atoms, as shown in Fig. 5a. This generally suggests the propensity of these Fe atoms to attract anions. Specifically focusing on the goethite surface without considering interfacial water (illustrated in red Fig. 5a), traversing away around the positions of Fe atoms results in a decrease in the electric potential and vice versa. However, for the entire system, i.e., in the goethite-water system, the electric potential progressively increases as moving from the bulk goethite toward the surface, with the highest potentials observed at the interface between the surface and water. Consequently, anions in the bulk water/solution are more likely to be strongly attracted to the surface due to the increasing positive potential. When moving from the goethite surface towards the bulk water and increasing the distance, the electric potential exhibits a linear increase, as depicted in Fig. 5a-b. This trend reflects the influence of the positively charged surface on the surrounding water molecules and the gradual

accumulation of positive charge density towards the bulk water. The corresponding electric field which is the negative gradient of the electric potential along the x-axis of the simulation box is presented in Fig. 5c-d. It is important to note that the electric field points away from positively charged objects and towards negatively charged objects, with its magnitude directly proportional to the rate of change of the electric potential. In this regard, interpreting these findings in terms of chemistry suggests that at the goethite-water interface or in its vicinity, an attractive electric potential (electric field) is generated, facilitating the adsorption of anions like phosphates and carboxylates onto the surface.

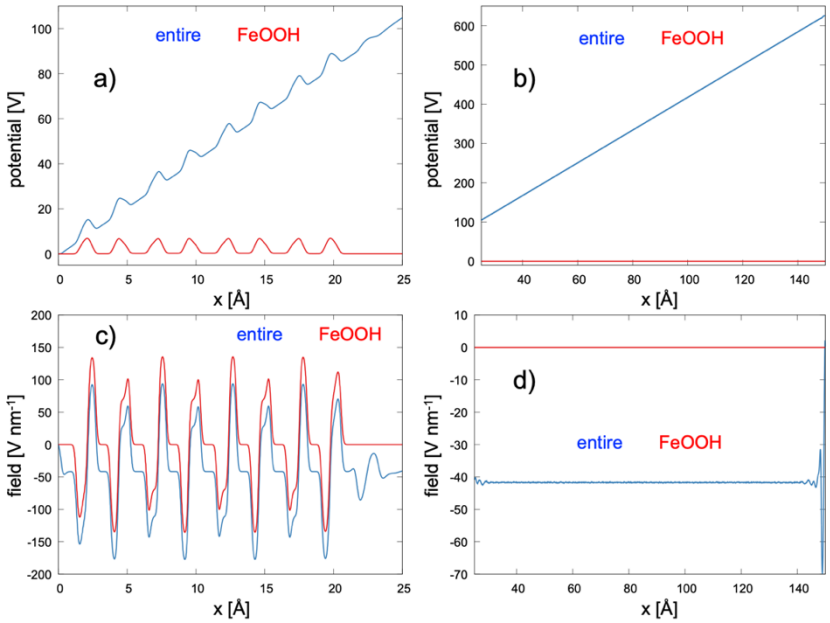

Figure 5. The electric potential and corresponding electric field along the axis perpendicular (x) to the interface for both the goethite surface (depicted in red) and the entire system (depicted in blue) at different distances within the simulation box.

3.2.2. Single-molecule adsorption at the goethite-water interface

Moving to scenarios involving the adsorption of single P (OP, GP, or IHP) or OM (CIT or HIS) at the goethite-water interface, no significant differences are observed in the characteristics of the goethite-water interface across these various situations when compared to the case of the bare goethite-water interface. This is evident from various calculated properties observed at both the interface and within the bulk water. For instance, one can examine the electric potential, electric field, and density profiles along the simulation box, as depicted in Fig. 6, along with the radial distribution function of water shown in Fig. 10. This indicates a negligible impact on the goethite-water interface in the presence of individual P or OM entities at the surface, irrespective of their size, charge, or any other physical or chemical attribute. As a result, the goethite surface within these interfaces particularly in the region of the Helmholtz layer would similarly promote the favorable adsorption of additional anions from the bulk water, akin to the behavior observed at the bare goethite-water interface.

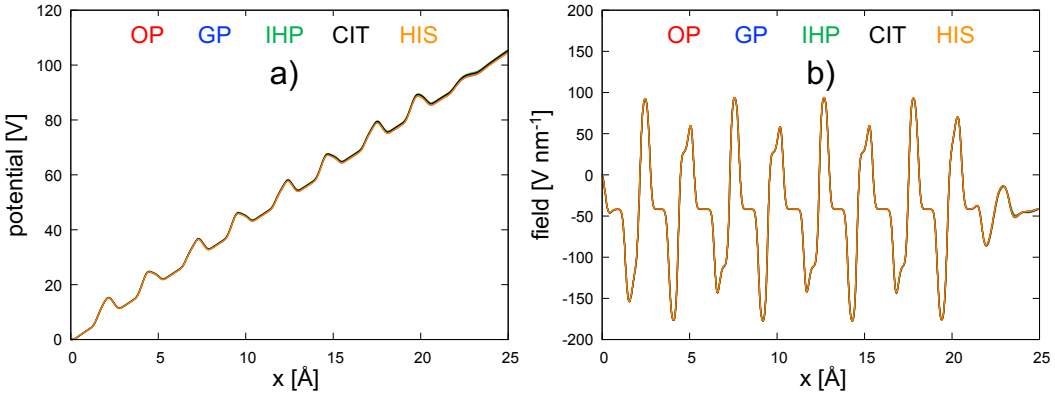

Figure 6. The electric potential (a) and electric field (b) along the axis perpendicular (x) to the interface for the entire system within the simulation box. These MD simulations involve the individual adsorption of every single P (OP, GP, or IHP) or OM (CIT or HIS) molecule at the goethite surface.

Regarding the binding of individual P and OM at the goethite-water interface, the dynamic configurations during the MD simulations, the center of mass motion and partial density along the simulation box perpendicular to the interface, minimum distance from the surface, and interaction energy and its contributing components, as well as hydrogen bonding with the surface and water, will be presented and discussed in the following sections.

The dynamic behavior of OP, GP, IHP, CIT, and HIS binding at the goethite-water interface was investigated using MD simulations over a 20 ns period for each case. Fig. 7 presents overlays of 100 snapshots taken at equidistant time intervals during the simulations, providing insights into the binding dynamics of these molecules. In addition, individual snapshots along the MD simulations showing the dynamic behavior of P and OM are provided in the supporting information, see Figs. S5-S9. Figures 7a-d depict the binding behavior of OP and GP, showing that they initially bind to the goethite surface at the start of the simulations before diffusing towards the water bulk, suggesting a weak binding affinity to the surface. In contrast, both IHP and CIT (Fig. 7e-h and 7m-p) exhibit close contact with the surface and movement at the surface along its plane throughout the simulation duration, without diffusing into the bulk water. This suggests a strong binding affinity of IHP and CIT to the goethite surface. Additionally, HIS displays an intermediate behavior, remaining in close contact with the surface for more than half of the simulation time before exhibiting diffusion back and forth between the surface and the water bulk, see Fig. 7i-l. This suggests an intermediate binding affinity of HIS to the goethite surface, falling between the weakly bound cases of OP and GP and the strongly bound cases of IHP and CIT.

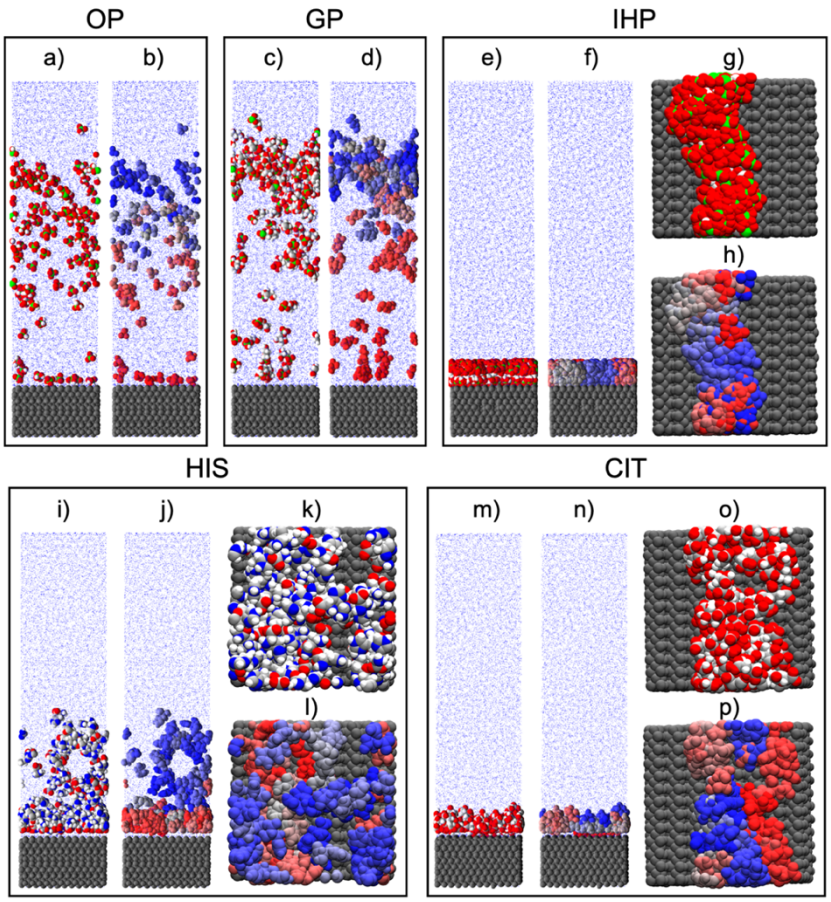

Figure 7. Overlays of 100 snapshots captured at equidistant time intervals during MD simulations depicting the adsorption of each OP, GP, IHP, CIT, and HIS at the goethite surface. Side view overlays are provided for OP ((a) and (b)) and GP ((c) and (d)), while both side and top views are presented for the strongly bound IHP (side: (e) and (f), and top: (g) and (h)), HIS (side: (i) and (j), and top: (k) and (l)), and CIT (side: (m) and (n), and top: (o) and (p)). Each P and OM is represented in two styles. First ((a), (c), (e), (g), (i), (k), (m), and (o)), atoms are color-coded: H, C, N, O, and P atoms are portrayed in white, red, gray, blue, and green, respectively. Second ((b), (d), (f), (g), (i), (l), (n), and (p)), P and OM molecules transition from red (start of the simulation: 0 ns) to blue (end of the simulation: 20 ns), illustrating the dynamic behavior of P and OM at the goethite surface throughout the MD simulation.

The observed binding tendencies of P and OM to the goethite surface, as discussed earlier, are corroborated by analyzing the calculated center of mass (COM) motion of OP, GP, IHP, CIT, and HIS along the x-axis of the simulation box throughout the MD simulation. The COM motion reveals an intermediate level of movement for HIS along the x-axis compared to a higher degree of motion for OP and GP, and a lower degree for IHP and CIT, as depicted in Fig. S10a-b in the supporting information. The trend in COM motion follows the sequence: IHP < CIT < HIS < OP < GP. This hierarchy suggests a binding affinity of the goethite surface to P and OM that increases in the order of GP < OP < HIS < CIT < IHP.

Furthermore, a similar trend was observed for the calculated minimum distances between each P or OM molecule and the goethite surface. In essence, these minimum distances provide insights into the proximity and interactions among different components of the molecular system throughout the simulation. Specifically, the minimum distance increased along the MD simulation in the sequence: IHP < CIT < HIS < OP < GP, as illustrated in Fig.

S10c-d in the supporting information. In the same context, distributions of each P and OM, along with accompanying Na^+ ions, along the x-axis of the simulation box are illustrated in Fig. 8 through their partial densities. Fig. 8a reveals that during the MD simulation trajectory, IHP, CIT, and HIS are predominantly located near the goethite surface, indicating their high affinity to bind to the surface. While both OP and GP exhibit peaks in proximity to the surface, their presence extends into the bulk water, suggesting a lower affinity to bind to the surface, particularly for GP. The partial densities of Na^+ ions accompanying P and OM confirm this observed behavior, see Fig. 8b. In conclusion, all these observations align consistently, indicating a rise in the binding affinity of the goethite surface to P and OM in the sequence: GP < OP < HIS < CIT < IHP, as evidenced by Figs. 7-8 and Fig. S10 in the supporting information.

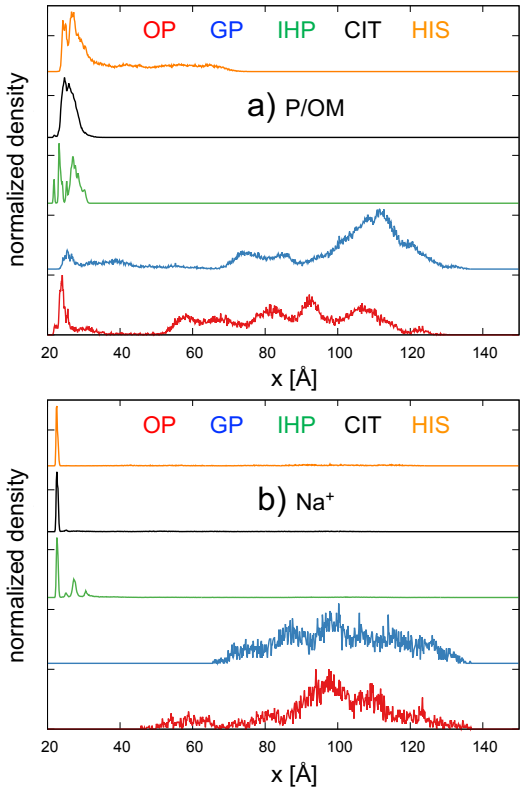

Figure 8. The partial density of each OP, GP, IHP, CIT, and HIS (a), along with their corresponding accompanying Na^+ ions (b), along the axis perpendicular (x) to the interface throughout the entire simulation box. These MD simulations correspond to the individual adsorption of each OP, GP, IHP, CIT, and HIS at the goethite surface. Note: partial density indicates the probability of finding a particular particle in space.

In terms of the interactions within each P/OM-goethite-water molecular model involving all components, our simulations indicate nearly identical water-water interactions with no significant variations observed among the molecular models containing P (OP, GP, and IHP) and OM (CIT and HIS) at the goethite-water interface, as depicted in the radial distribution function and the distribution of hydrogen bonds (HBs) in Fig. 9a-b. Here, water-water HBs are characterized as moderately strong, predominantly electrostatic, with donor-acceptor (D-A)

distances ranging from 2.4 to 3.6 Å, centered around a maximum of 2.8 Å. Similarly, almost identical HBs with consistent strength and distribution are observed between the goethite surface and interfacial water molecules, see Fig. 9d. Nevertheless, contrary to the HBs observed between water molecules (water-water) and those formed between goethite and water (goethite-water), all P and OM species investigated in this study exhibit stronger HBs with water molecules, as depicted in Fig. 9c. Notably, among these species, IHP displays the most robust HBs, followed by CIT and OP, while GP and HIS demonstrate relatively weaker interactions. Specifically, the distributions of HBs observed for P and OM with water reveal peaks of D-A distances, with maxima at 2.62 Å for IHP, 2.68 Å for both OP and CIT, with CIT having higher intensity, and 2.73 Å for both GP and HIS, with GP displaying relatively higher intensity. Furthermore, the total number of HBs observed during the MD simulation for P and OM with water is tallied at each time step, as depicted in Fig. S8 in the supporting information. On average, the number of these HBs fluctuates around 8.9 for OP, 11.0 for GP, 11.1 for HIS, 14.7 for CIT, and 29.4 for IHP. Analyzing the combination of the number of HBs with their strength reveals the highest affinity of IHP in its interaction with water, an intermediate affinity for CIT, and the lowest affinity for GP, HIS, and OP, particularly for the OP case. This finding aligns with the calculated interaction energy of each P or OM with the surrounding water molecules within a range of 11 Å, as depicted in Fig. 10. Eventually, all the observed HBs at the goethite-water interface in the presence of P and OM come in accord with the FTIR observations by Norén and Persson (2007) that highlighted the significant role of the HBs in the binding process at the goethite-water interface.

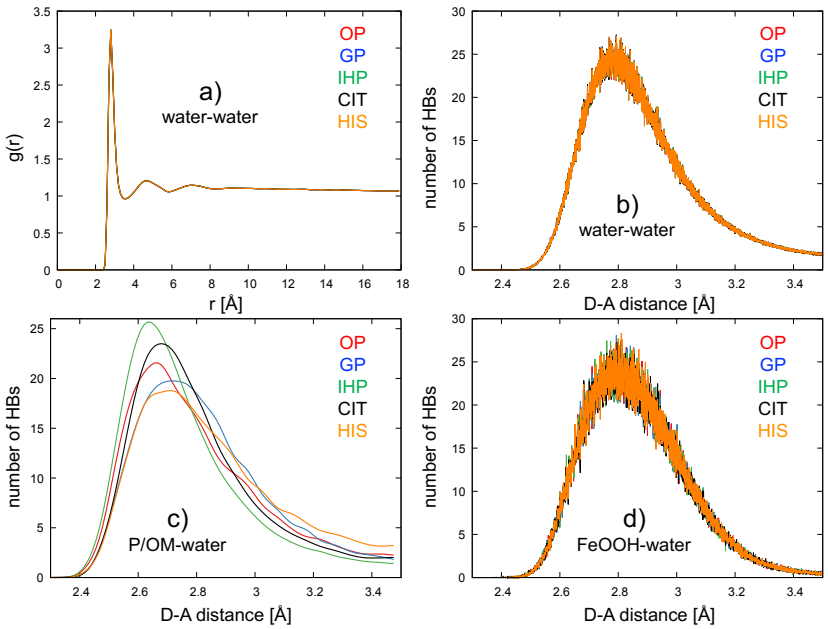

Figure 9. The radial distribution function of water (a) and the number of hydrogen bonds (HBs) within water (b), between water and each of P and OM (c), and between the goethite surface and water (d) for the adsorption of each OP, GP, IHP, CIT, and HIS at the goethite surface.

In terms of the interaction of P compounds (OP, GP, and IHP) and OM (CIT and HIS) with the goethite surface, the calculated interaction energies follow the order: GP < OP < HIS < CIT < IHP (refer to Fig. 10a-b). This hierarchy elucidates that among the P compounds, IHP exhibits stronger binding to the goethite surface compared to OP, while OP demonstrates stronger binding than GP. This observation is consistent with our previous quantum mechanics/molecular mechanics (QM/MM) results (Ganta et al., 2021), which also indicate a similar order of P binding affinity towards goethite. Furthermore, these findings are consistent with the results of current adsorption experiments involving OP, GP, and IHP at the goethite surface under diverse experimental conditions, which suggest a binding/adsorption hierarchy of GP < OP < IHP, as illustrated in Figs. 2a, 3a, and Figs. S1-S2 in the supporting information. It is worth highlighting that electrostatic Coulomb interactions predominantly contribute to the total interaction energies reported in Fig. 10, in contrast to the dispersion (in this case, Lennard Jones, LJ) interaction energy, see Figs. S12-S13 in the supporting information. This predominance primarily stems from the repulsive component outweighing the attractive part of the LJ potential in the interaction between each P or OM and the goethite surface. This occurrence arises from the proximity of both P and OM compounds to the goethite surface, resulting in positive dispersion interaction energy. GP exhibits exceptional behavior, as depicted in Fig. S13 in the supporting information, owing to its relatively distant positioning from the surface, as illustrated in Figs. 7-8. This results in the prevalence of dispersion interactions over electrostatic interactions, thereby contributing to the relative stability of GP at the surface.

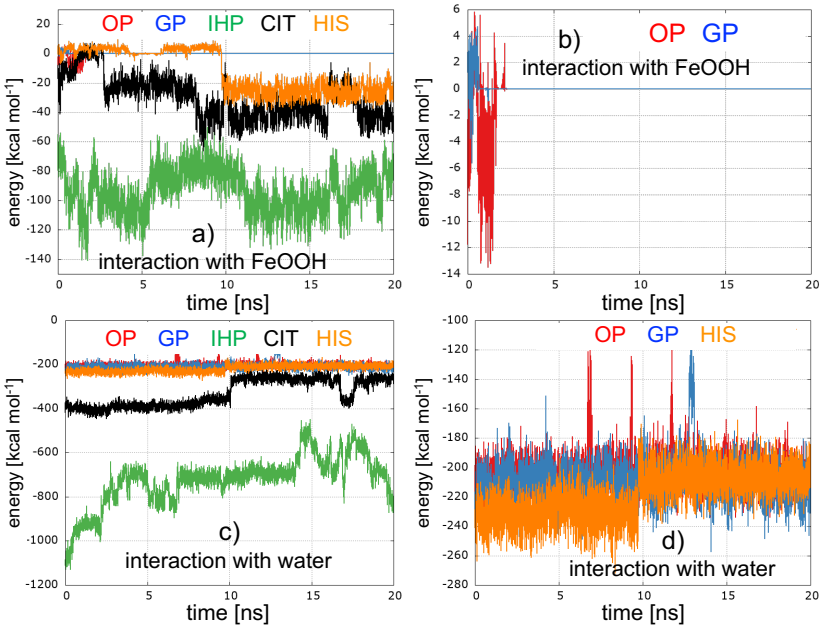

Figure 10. The total interaction energy (combining electrostatic and dispersion contributions) of each P (OP, GP, and IHP) and OM (CIT and HIS) with both the goethite surface (a-b) and water (c-d) throughout the MD simulation. Additionally, Fig. S14 in the supporting information shows the interaction energy of both OP and GP with the surface within the first 2.5 ns of the MD simulation.

The prevalence of electrostatic Coulomb interactions was also observed in the interaction energy between each P or OM and water. The total interaction energy of P compounds (OP, GP, and IHP) and OM (CIT and HIS) with water exhibited a similar order to that observed with the goethite surface, with the order being: OP ≤ GP < HIS < CIT < IHP (refer to Fig. 10c-d). These electrostatic interactions are corroborated by the number of HBs observed for P and OM with water, following the order: OP < GP < HIS < CIT < IHP (see Fig. S11 in the supporting information), along with the strength of the HBs shown in Fig. 9c, as discussed earlier.

Regarding the effect of OM on the P binding at the goethite surface, the interaction energy showed that both CIT and HIS display stronger binding to goethite compared to OP and GP, see Fig. 10a. This implies that CIT and HIS possess the capability to displace OP and GP from the goethite surface competitively. Consequently, coating the surface with CIT or HIS could impede the adsorption of OP and GP by blocking the active sites at the goethite surface, thereby promoting their desorption and mobilization processes. This elucidates why CIT and HIS can impede the P adsorption, particularly for GP and OP, as observed in the present experiments, see Fig. 2b-c and Fig. 3b-c. This inhibitory effect is more pronounced in the case of CIT due to its superior adsorption (and interaction energy with the goethite surface) thus blocking more active sites at the goethite surface compared to HIS. This finding concurs with the present experimental results and clarifies why CIT exerts a potent inhibitory effect on P binding to the goethite surface.

In the case of IHP, its adsorption on the goethite surface covered with OM (CIT or HIS) remains largely unaffected due to its stronger binding affinity to the goethite surface compared to both CIT and HIS, see Fig. 10a. This strong affinity allows IHP not only to be influenced by OM but also positions it as a strong competitor, potentially reducing the binding affinity of CIT and HIS and replacing them at the surface. This explains the experimental observation of minimal changes in the impact of OM on IHP adsorption, see Fig. 2d and Fig. 3d. Despite being relatively minor in affecting IHP adsorption, the more noticeable decrease in IHP adsorption observed when the surface is covered with CIT compared to HIS can be attributed to the more pronounced inhibitory effect of CIT compared to HIS. This can be traced back to the stronger binding and higher affinity of CIT to the surface compared to HIS, as discussed earlier in the context of the OP and GP cases.

3.2.3. Covering the goethite surface with OM

To delve deeper into the impact of OM on the P binding process at the goethite surface, we constructed two models featuring goethite surfaces covered with a monolayer of either CIT or HIS. Each model included 38 individual molecules (anions) of CIT or HIS to form the monolayer. To counterbalance the negative charge from the HIS (-38) and CIT (-78) molecules, an equivalent number of sodium ions (Na^+) was introduced into each simulation box, which spanned 150 Å perpendicular to the goethite-water interface. The overlay of snapshots captured during MD simulations of the goethite surface covered with HIS and CIT individually is depicted in Fig. 11. These simulations reveal that the majority of HIS and CIT molecules tend to adhere to the surface, forming monolayers that cover and block all active

sites at the surface. Consequently, this diminishes the likelihood of anions such as phosphates being adsorbed at the surface in the presence of the formed OM monolayer. According to these MD simulations, approximately 34-35 CIT molecules remain adsorbed at the surface, with about 3-4 molecules diffusing into the bulk water during the simulation. Conversely, in the case of HIS, around 28 molecules remain adsorbed at the surface, while approximately 10 molecules diffuse into the bulk water throughout the simulation. Once again, this underscores the strong affinity of CIT to bind to the goethite surface compared to HIS, with electrostatic interactions playing a significant role. Moreover, upon the formation of monolayers of OM (CIT and HIS) on the goethite surface, dissolution of the goethite surface was observed along the MD simulation, especially for the CIT case, see the dissolved gray goethite atoms in Fig. 11. In addition to enhancing the phosphate mobility, this surface dissolution process comes in accord with the surface dissolution observed in the literature, e.g., see (Duckworth and Martin, 2001; Guppy et al., 2005; Han et al., 2020).

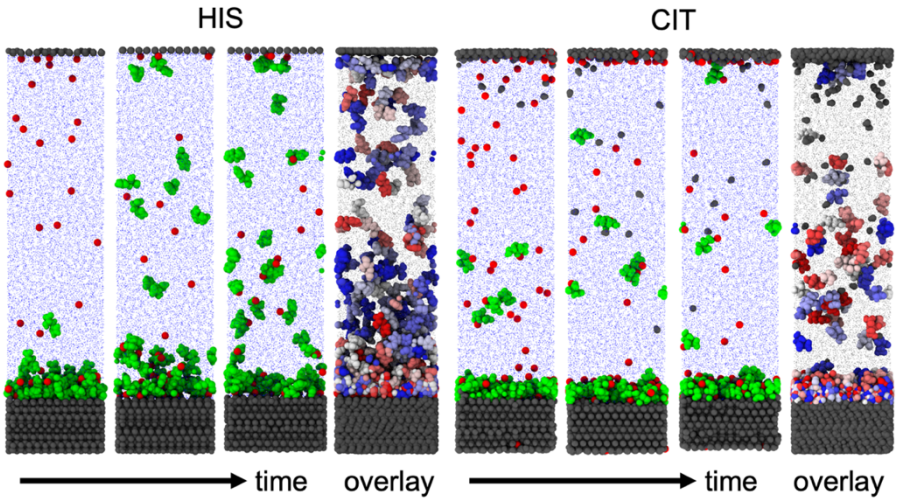

Figure 11. Snapshots taken during MD simulations showing the dynamic behavior of the goethite surface covered with a monolayer of 38 HIS molecules (left 4 panels) and 38 CIT molecules (right 4 panels). The first three left configurations/panels of each case, namely HIS and CIT, depict the specific arrangement, with HIS and CIT molecules colored in green, goethite in gray, Na^+ ions in red, and water in blue points. Additionally, overlays of snapshots captured during MD simulations illustrate the evolving behavior of these two cases. In the overlays, CIT and HIS molecules transition from red (start of the simulation: 0 ns) to blue (end of the simulation: 20 ns), while goethite remains in gray.

In terms of the electrostatic effect, the electric potential along the x-axis exhibits negative values, primarily attributed to the accumulation of negatively charged OM molecules forming the monolayer at the surface, alongside the diffusion of some molecules into the bulk water, as discussed previously. Figure 12 illustrates peaks indicating maximum positive charge densities observed at the positions of Fe atoms. This electric potential gradually decreases to more negative values when moving from the bulk goethite towards the surface, with the lowest potentials observed at the interface between the surface and water. Consequently, anions present in the bulk water or solution are unlikely to bind to the surface due to the increasing negative potential. This highlights the pivotal role played by both CIT and HIS as inhibitors in the P-binding process. It elucidates the experimental finding regarding the substantial influence of OM on P adsorption, particularly when the goethite surface is pre-covered with

OM before the adsorption process, notably in cases involving OP and GP, as depicted in Fig. 2b-c and Fig. 3b-c.

Furthermore, the observed negative potential for goethite covered with OM aligns with the expectations proposed by (Sibanda and Young, 1986) and (Fu et al., 2013). They suggested that an unfavorable electrostatic potential or field could be generated around the adsorbed humic acid molecules, potentially hindering P adsorption. While comparing the outcomes of the present study with those of others who have applied humic substances (HSs), such as (Sibanda and Young, 1986) and (Fu et al., 2013), it is important to highlight that the HSs are not as pure as the OM applied in the present study. Typically, all HSs contain some minerals, such as metal ions/clusters/colloids, which are likely predominantly composed of Al and Fe. However, the key distinction lies in the composition of OM utilized in our study, particularly at high surface coverage, compared to the HSs (HA and FA) which have a higher concentration of carboxylate and hydroxyl groups. These groups enhance the negative charge on the goethite surface, initiating discussions on the unfavorable electric potential and field at the surface.

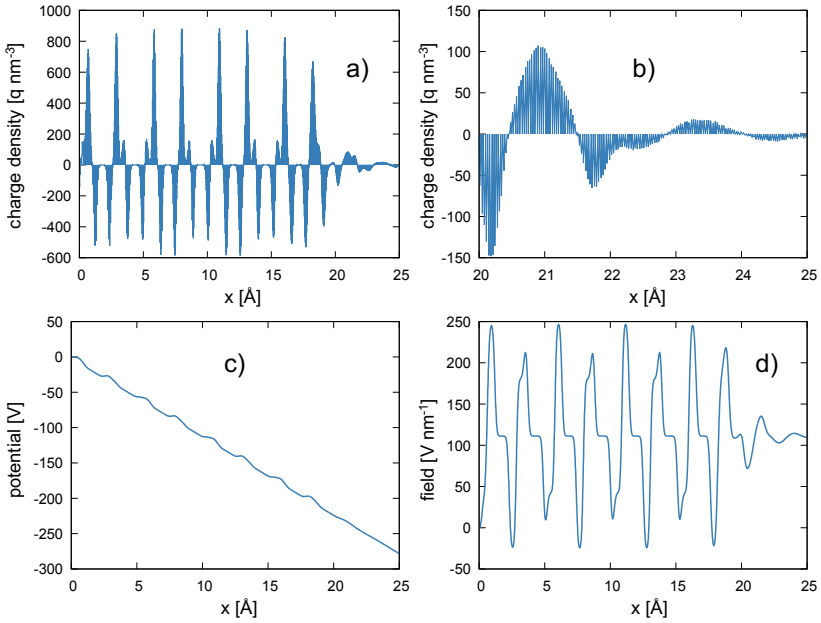

Figure 12. The distribution of charge density (a-b), electric potential (c), and electric field (d) along the axis perpendicular (x) to the interface of the entire system for the goethite surface covered with a monolayer of 38 HIS molecules. For comparison with the interface between the bare goethite surface and water, see Fig. S15 in the supporting information.

3.2.4. Co-adsorption at the goethite-water interface

To examine how OM affects the GP binding process at the goethite surface in the co-adsorption scenario, we developed two models incorporating CIT or HIS separately on goethite surfaces alongside GP. For each model (GP-CIT and GP-HIS), two initial configurations were established. In one configuration, the combination of GP with each OM (CIT or HIS) was positioned on the surface, while in the second configuration, the combination

was situated in the bulk water, far from the surface. For both configurations (whether on the surface or in the bulk water), the formation of stable complexes between GP and both HIS and CIT individually was observed during the MD simulation. For instance, Fig. 13a-b illustrates the interaction between GP and each of CIT and HIS at some periods along the MD simulation trajectory.

Furthermore, it was noted that GP exhibited stronger binding and interaction energy with the goethite surface in the presence of CIT and HIS compared to when GP was alone, see Fig. 13a-d. These observations align with experimental findings indicating that the surface prefers binding GP in the presence of HIS and CIT in the co-adsorption scenario compared to when GP is alone, see Fig. 2c, Fig. 3c, and Fig. 13a-d. Despite CIT binding relatively more strongly to the surface than HIS, GP demonstrates stronger binding in the presence of HIS compared to the CIT case due to the formation of a more stable complex between GP and HIS, see Fig. 13a-c. As a result, the more stable GP-HIS complex exhibits stronger binding to the goethite surface compared to the GP-CIT complex, ultimately leading to enhanced GP adsorption in the presence of HIS. This finding confirms our interpretation of the present experiments of the formation of GP-OM complexes, which result in higher adsorption compared to the scenario where GP is alone.

Although the co-adsorption of GP in the presence of HIS enhanced GP adsorption, intriguingly, IHP demonstrated lower binding to the surface in the presence of HIS compared to bare IHP adsorption, as depicted in Fig. 13e-f. This is evidenced by the lower interaction energy between IHP and the surface observed in Fig. 13e, compared to that for bare IHP adsorption, i.e., adsorption of IHP in the absence of OM. These findings are consistent with present experimental observations regarding the effect of OM on IHP adsorption in the co-adsorption scenario. This reduced interaction is attributed to the weakened interaction between IHP and the surface, as well as the distance between IHP and the surface observed at certain intervals during the MD simulation. This can be understood by observing a second peak of the partial density for IHP in the presence of HIS at around 30 Å, far from the goethite surface, as shown in Fig. 13f. This aspect is also evident from Fig. 14, which illustrates the dynamic behavior of the co-adsorption of IHP with HIS at the goethite surface, showing instances where IHP moves away from and returns to the surface.

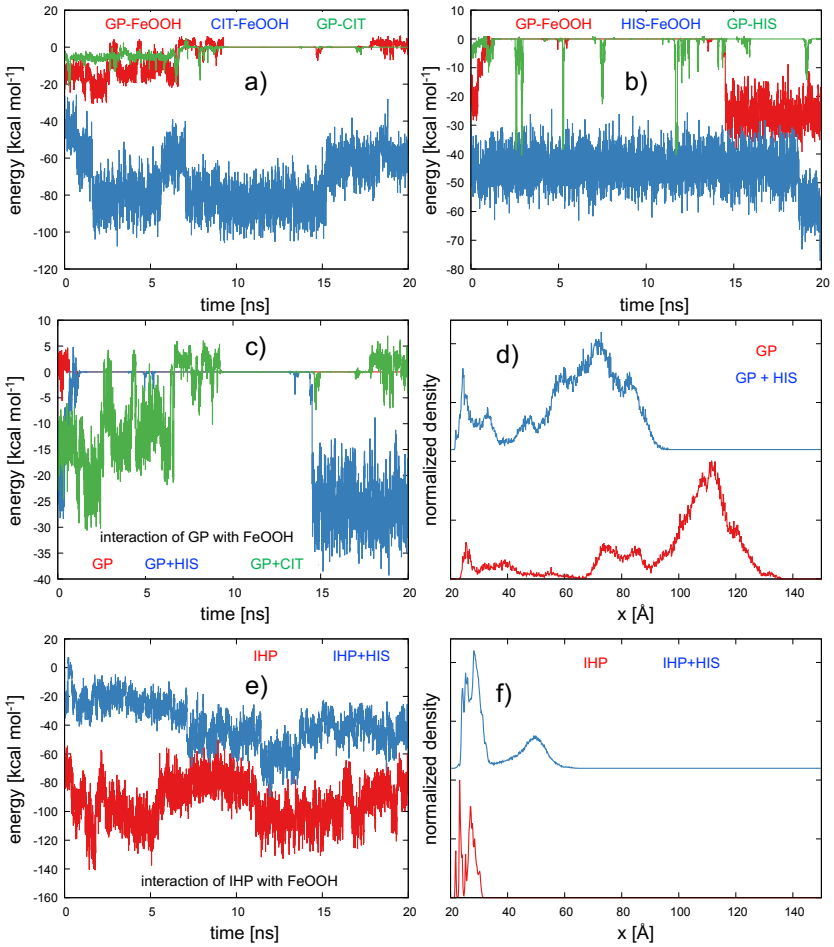

Figure 13. The total interaction energy (comprising both electrostatic and dispersion components) during the MD simulation of GP co-adsorption with CIT (a) and HIS (b). In these panels, GP-FeOOH, CIT-FeOOH, GP-CIT, HIS-FeOOH, and GP-HIS denote the interaction energy between each pair of components, where, for instance, GP-FeOOH represents the interaction between GP and the goethite surface. Additionally, panels (c) and (d) illustrate the influence of OM on GP in the co-adsorption scenario through the interaction energy (c) and partial density along the axis perpendicular (x) to the interface throughout the entire simulation box (d). Similarly, panels (e) and (f) demonstrate the impact of HIS on IHP in the co-adsorption scenario via the interaction energy (e) and partial density (f). Here, GP+HIS and GP+CIT signify GP in the presence of HIS and CIT, respectively, with the same notation applying to IHP.

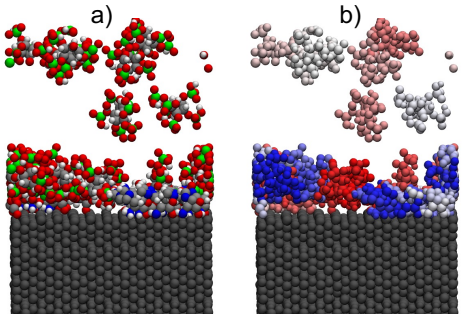

Figure 14. Overlays of snapshots captured during MD simulations depict the evolving behavior of IHP adsorption in the presence of HIS in the co-adsorption scenario. In panel (e), atoms are color-coded as follows: white (H), red (O), blue (N), silver (C), green (P), and gray (representing the entire goethite). In panel (f), IHP and HIS molecules transition from red (start of the simulation: 0 ns) to blue (end of the simulation: 20 ns), while the goethite remains depicted in gray. Water molecules are excluded from visualization for clarity.

4. Summary

In summary, the present contribution offers a molecular-level perspective on how organic matter (OM) influences phosphorus (P) binding/adsorption at the goethite-water interface through a combined experimental-theoretical approach. We examined the impact of citric acid (CIT) and histidine (HIS) treatments on the adsorption of orthophosphate (OP), glycerolphosphate (GP), and inositolhexaphosphate (IHP). Our experimental findings highlight the complexity of P adsorption on goethite, showing its dependence on the chemical structure of both P and OM, treatment conditions, and initial P concentrations.

Notably, IHP consistently exhibits the highest affinity for goethite, while GP shows the lowest. OP is highly sensitive to OM inhibition, especially when covering the surface with CIT, resulting in a 70% reduction in the adsorption capacity. Conversely, IHP displays less sensitivity, with a 20% reduction with CIT coverage. GP demonstrates intermediate inhibition, with a 31% reduction with HIS coverage. In contrast, covering the surface with the other OM results in a 60% reduction for OP with HIS, 6% for IHP with HIS, and 13% for GP with CIT. Simultaneous co-adsorption of OM with OP and IHP induces similar inhibitions, with reductions of 54% for OP and 10% for IHP. This highlights the significant inhibition caused by the prior surface coating with OM, particularly CIT, with no significant difference observed between CIT and HIS in the co-adsorption scenario. Surprisingly, co-adsorption of OM with GP leads to increased adsorption capacity, by 47% for CIT and 38% for HIS, respectively.

The present molecular modeling results shed light on the behavior of the Helmholtz layer at the goethite-water interface. Specifically, at low surface loading and in the absence of P and OM, the interface demonstrates a favorable electric potential and electric field. This favorable electrostatic environment within the Helmholtz layer facilitates the adsorption of anions such as phosphates and carboxylates onto the goethite surface. Consequently, these findings provide a compelling explanation for all experimental observations concerning the intrinsic affinity of bare goethite for adsorbing these anions, rooted in the electrochemical dynamics of the Helmholtz layer. This phenomenon extends to goethite surfaces loaded with low P and OM concentrations, supporting further anion adsorption. Moreover, the results indicate an intermediate binding affinity of HIS to the goethite surface, falling between weakly bound OP and GP and strongly bound IHP and CIT, with the sequence of goethite binding affinity to P and OM as follows: GP < OP < HIS < CIT < IHP. The order of P binding aligns with our experimental findings, elucidating the increasing P adsorption trend: GP < OP < IHP.

Furthermore, our results demonstrate that both CIT and HIS exhibit stronger binding to goethite than OP and GP, leading to competition and subsequent inhibition of OP and GP adsorption. When CIT and HIS pre-cover the surface, they block active sites and inhibit OP and GP adsorption, with CIT showing a more pronounced inhibitory effect due to its superior binding at the goethite surface. Additionally, the covered surface with OM presents an unfavorable negative electric potential at the interface, further hindering P adsorption. This finding corroborates our experimental results, explaining the inhibitory effect of OM, particularly CIT, on P adsorption. Furthermore, this elucidates all experimental observations

concerning the inhibitory effect on the adsorption of anions at a surface already pre-covered with adsorbed anions.

Despite the general inhibitory effect of OM, its presence in solution with GP enhances GP binding to the goethite surface, as observed in the co-adsorption scenario. This enhancement stems from the formation of GP-OM complexes with a higher affinity for goethite surfaces compared to individual GP adsorption, consistent with our experimental findings. Moreover, the stronger binding of the GP-HIS complex to the goethite surface compared to the GP-CIT complex ultimately enhances GP adsorption in the presence of HIS, confirming and explaining the experimental finding relevant to the observed potential effect of GP adsorption enhancement, particularly with HIS.

Although our study focused solely on two organic molecular systems (HIS and CIT), our findings have significant potential for generalization. This is because our research demonstrates the consistent behavior of CIT and HIS (organic acids) across diverse conditions, including surface coverage, co-adsorption, and adsorption of various phosphate species (OP, GP, and IHP). Moreover, our results are consistent with prior research conducted on similar and different minerals, as well as whole soil samples. Additionally, the inclusion of mechanistic insights through MD simulations enhances the reliability of our conclusions. While we acknowledge potential limitations, further validation, and exploration could undoubtedly improve the applicability of our findings.

In conclusion, our study offers crucial insights into the molecular-level influence of OM on P binding at the surface, impacting P mobility and soil fertility, which is pivotal for sustaining a growing human population. However, several challenges and open issues persist in the dynamics of P adsorption and release. These include exploring OM variants with more carboxylate functional groups, investigating aromatic OM with carboxylate functional groups as well as applying naturally humic substances, examining the effects of electrolytes and ionic strength, understanding the role of inorganic anions, characterizing P and OM binding at the goethite-water interface, and assessing the consequences of sequential adsorption by P and OM. Addressing these inquiries will not only deepen our understanding of complex interactions among P, OM, and mineral surfaces but also provide valuable insights into P fate and transport in natural settings. Through interdisciplinary approaches integrating experimental and theoretical methodologies, we can advance our understanding and contribute to the development of more sustainable soil fertility management strategies and environmental conservation practices.

Credit authorship contribution statement

Ashour A. Ahmed is credited with conceptualization, conducting the modeling work, all experimental and modeling analysis and interpretation, methodology development, visualization, and writing the original manuscript. Mohsen Morshedizad conducted the sorption experiments. Ashour A. Ahmed, Oliver Kühn, and Peter Leinweber are responsible for funding acquisition, reviewing, and editing the manuscript. All authors have reviewed and approved the submitted version of this manuscript.

Funding

This research belongs mainly to the InnoSoilPhos project, funded by the German Federal Ministry of Education and Research (BMBF) in the frame of the BonaRes program (No. 031A558).

Declaration of competing interest

The authors declare no conflict of interest. The funders had no role in the design of the study; in the collection, analyses, or interpretation of data; in the writing of the manuscript, or in the decision to publish the results.

5. References

Abraham, M.J., Murtola, T., Schulz, R., Páll, S., Smith, J.C., Hess, B., Lindahl, E., 2015. GROMACS: High performance molecular simulations through multi-level parallelism from laptops to supercomputers. SoftwareX 1–2, 19–25. https://doi.org/10.1016/j.softx.2015.06.001

Ahmed, A.A., Gros, P., Kühn, O., Leinweber, P., 2018a. Molecular level investigation of the role of peptide interactions in the glyphosate analytics. Chemosphere 196, 129–134. https://doi.org/10.1016/j.chemosphere.2017.12.162

Ahmed, A.A., Gypser, S., Freese, D., Leinweber, P., Kühn, O., 2020. Molecular level picture of the interplay between pH and phosphate binding at the goethite–water interface. Phys. Chem. Chem. Phys. 22, 26509–26524. https://doi.org/10.1039/D0CP04698A

Ahmed, A.A., Gypser, S., Leinweber, P., Freese, D., Kühn, O., 2019. Infrared spectroscopic characterization of phosphate binding at the goethite–water interface. Phys. Chem. Chem. Phys. 21, 4421–4434. https://doi.org/10.1039/C8CP07168C

Ahmed, A.A., Kühn, O., Aziz, S.G., Hilal, R.H., Leinweber, P., 2014. How soil organic matter composition controls hexachlorobenzene–soil-interactions: Adsorption isotherms and quantum chemical modeling. Sci. Total Environ. 476–477, 98–106. https://doi.org/10.1016/j.scitotenv.2013.12.096

Ahmed, A.A., Leinweber, P., Kühn, O., 2023. Advances in understanding the phosphate binding to soil constituents: A Computational Chemistry perspective. Sci. Total Environ. 887, 163692. https://doi.org/10.1016/j.scitotenv.2023.163692

Ahmed, A.A., Leinweber, P., Kühn, O., 2018b. Unravelling the nature of glyphosate binding to goethite surfaces by ab initio molecular dynamics simulations. Phys. Chem. Chem. Phys. 20, 1531–1539. https://doi.org/10.1039/C7CP06245A

Ahmed, A.A., Thiele-Bruhn, S., Aziz, S.G., Hilal, R.H., Elroby, S.A., Al-Youbi, A.O., Leinweber, P., Kühn, O., 2015. Interaction of polar and nonpolar organic pollutants with soil organic matter: sorption experiments and molecular dynamics simulation. Sci. Total Environ. 508, 276–87. https://doi.org/10.1016/j.scitotenv.2014.11.087

Amadou, I., Faucon, M.-P., Houben, D., 2022. Role of soil minerals on organic phosphorus availability and phosphorus uptake by plants. Geoderma 428, 116125. https://doi.org/10.1016/j.geoderma.2022.116125

Andersen, D.S., Helmers, M.J., Burns, R.T., 2015. Phosphorus Sorption Capacity of Six Iowa Soils before and after Five Years of Use as Vegetative Treatment Areas. Appl. Eng. Agric. 611–620. https://doi.org/10.13031/aea.31.11128

Antelo, J., Arce, F., Avena, M., Fiol, S., López, R., Macías, F., 2007. Adsorption of a soil humic acid at the surface of goethite and its competitive interaction with phosphate. Geoderma 138, 12–19.

Antelo, J., Avena, M., Fiol, S., López, R., Arce, F., 2005. Effects of pH and ionic strength on the adsorption of phosphate and arsenate at the goethite–water interface. J. Colloid Interface Sci. 285, 476–486. https://doi.org/10.1016/j.jcis.2004.12.032

Arai, Y., Sparks, D.L., 2007. Interactions between phosphate and iron oxide, in: Advances in Agronomy. Elsevier, pp. 135–179. https://doi.org/10.1016/S0065-2113(06)94003-6

Arai, Y., Sparks, D.L., 2001. ATR–FTIR Spectroscopic Investigation on Phosphate Adsorption Mechanisms at the Ferrihydrite–Water Interface. J. Colloid Interface Sci. 241, 317–326. https://doi.org/10.1006/jcis.2001.7773

Arroyave, J.M., Puccia, V., Zanini, G.P., Avena, M.J., 2018. Surface speciation of phosphate on goethite as seen by InfraRed Surface Titrations (IRST). Spectrochim. Acta. A. Mol. Biomol. Spectrosc. 199, 57–64. https://doi.org/10.1016/j.saa.2018.03.043

Barrow, N., Bowden, J., Posner, A., Quirk, J., 1980. Describing the effects of electrolyte on adsorption of phosphate by a variable charge surface. Soil Res. 18, 395. https://doi.org/10.1071/SR9800395

Bellier, N., Chazarenc, F., Comeau, Y., 2006. Phosphorus removal from wastewater by mineral apatite. Water Res. 40, 2965–2971. https://doi.org/10.1016/j.watres.2006.05.016

Berendsen, H.J.C., Grigera, J.R., Straatsma, T.P., 1987. The missing term in effective pair potentials. J. Phys. Chem. 91, 6269–6271. https://doi.org/10.1021/j100308a038

Borggaard, O.K., 2001. Soil chemistry in a pedological context, 5. rev. ed. ed. Royal Veterinary and Agricultural University, København.

Borggaard, O.K., Raben-Lange, B., Gimsing, A.L., Strobel, B.W., 2005. Influence of humic substances on phosphate adsorption by aluminium and iron oxides. Geoderma 127, 270–279. https://doi.org/10.1016/j.geoderma.2004.12.011

Borggaard, O.K., Szilas, C., Gimsing, A.L., Rasmussen, L.H., 2004. Estimation of soil phosphate adsorption capacity by means of a pedotransfer function. Geoderma 118, 55–61. https://doi.org/10.1016/S0016-7061(03)00183-6

Boukemara, L., Boukhalfa, C., Reinert, L., Duclaux, L., 2016. Characterization of Phosphate Adsorption on Goethite Macroscopic and Spectroscopic Analyses. J. Mater. Environ. Sci. 7, 2541–2550.
Bussi, G., Donadio, D., Parrinello, M., 2007. Canonical sampling through velocity rescaling. J. Chem. Phys. 126, 014101. https://doi.org/10.1063/1.2408420
Chitrakar, R., Tezuka, S., Sonoda, A., Sakane, K., Ooi, K., Hirotsu, T., 2006. Phosphate adsorption on synthetic goethite and akaganeite. J. Colloid Interface Sci. 298, 602–608. https://doi.org/10.1016/j.jcis.2005.12.054
Cornell, R.M., Schwertmann, U., 2003. The iron oxides: structure, properties, reactions, occurrences, and uses, 2nd, completely rev. and extended ed ed. Wiley-VCH, Weinheim.
Cygan, R.T., Liang, J.-J., Kalinichev, A.G., 2004. Molecular Models of Hydroxide, Oxyhydroxide, and Clay Phases and the Development of a General Force Field. J. Phys. Chem. B 108, 1255–1266. https://doi.org/10.1021/jp0363287
Dakora, F.D., Phillips, D.A., 2002. Root exudates as mediators of mineral acquisition in low-nutrient environments. Plant Soil 245, 35–47. https://doi.org/10.1023/A:1020809400075
Debicka, M., Morshedizad, M., Leinweber, P., 2023. The Effects of Dissolved Organic Matter Derived from Agricultural Waste Materials on Phosphorus Sorption in Sandy Soils. Agriculture 13, 2164. https://doi.org/10.3390/agriculture13112164
Dimirkou, A., Ioannou, A., Doula, M., 2002. Preparation, characterization and sorption properties for phosphates of hematite, bentonite and bentonite–hematite systems. Adv. Colloid Interface Sci. 97, 37–61. https://doi.org/10.1016/S0001-8686(01)00046-X
Drouillon, M., Merckx, R., 2003. The role of citric acid as a phosphorus mobilization mechanism in highly P-fixing soils. Gayana Botánica 60. https://doi.org/10.4067/S0717-66432003000100009
Duckworth, O.W., Martin, S.T., 2001. Surface complexation and dissolution of hematite by C 1 -C 6 dicarboxylic acids at pH = 5.0. Geochim. Cosmochim. Acta 65, 4289–4301. https://doi.org/10.1016/S0016-7037(01)00696-2
Dultz, S., Steinke, H., Mikutta, R., Woche, S.K., Guggenberger, G., 2018. Impact of organic matter types on surface charge and aggregation of goethite. Colloids Surf. Physicochem. Eng. Asp. 554, 156–168. https://doi.org/10.1016/j.colsurfa.2018.06.040
Elzinga, E.J., Sparks, D.L., 2007. Phosphate adsorption onto hematite: an in situ ATR-FTIR investigation of the effects of pH and loading level on the mode of phosphate surface complexation. J. Colloid Interface Sci. 308, 53–70. https://doi.org/10.1016/j.jcis.2006.12.061
Freundlich, H., 1907. Über die Adsorption in Lösungen. Z. Für Phys. Chem. 57U. https://doi.org/10.1515/zpch-1907-5723
Fu, Z., Wu, F., Song, K., Lin, Y., Bai, Y., Zhu, Y., Giesy, J.P., 2013. Competitive interaction between soil-derived humic acid and phosphate on goethite. Appl. Geochem. 36, 125–131. https://doi.org/10.1016/j.apgeochem.2013.05.015
Furrer, G., Stumm, W., 1986. The coordination chemistry of weathering: I. Dissolution kinetics of δ-Al2O3 and BeO. Geochim. Cosmochim. Acta 50, 1847–1860. https://doi.org/10.1016/0016-7037(86)90243-7
Ganta, P.B., Kühn, O., Ahmed, A.A., 2020a. Ab Initio Molecular Dynamics Simulations of the Interaction between Organic Phosphates and Goethite. Molecules 26, 160. https://doi.org/10.3390/molecules26010160
Ganta, P.B., Kühn, O., Ahmed, A.A., 2020b. QM/MM Molecular Dynamics Investigation of the Binding of Organic Phosphates to the 100 Diaspore Surface. Front. For. Glob. Change 3. https://doi.org/10.3389/ffgc.2020.00071
Ganta, P.B., Kühn, O., Ahmed, A.A., 2019. QM/MM simulations of organic phosphorus adsorption at the diaspore–water interface. Phys. Chem. Chem. Phys. 21, 24316–24325. https://doi.org/10.1039/C9CP04032C
Ganta, P.B., Morshedizad, M., Kühn, O., Leinweber, P., Ahmed, A.A., 2021. The Binding of Phosphorus Species at Goethite: A Joint Experimental and Theoretical Study. Minerals 11, 323. https://doi.org/10.3390/min11030323
Gao, Y., Mucci, A., 2001. Acid base reactions, phosphate and arsenate complexation, and their competitive adsorption at the surface of goethite in 0.7 M NaCl solution. Geochim. Cosmochim. Acta 65, 2361–2378. https://doi.org/10.1016/S0016-7037(01)00589-0
Geelhoed, J.S., Hiemstra, T., Van Riemsdijk, W.H., 1998. Competitive Interaction between Phosphate and Citrate on Goethite. Environ. Sci. Technol. 32, 2119–2123. https://doi.org/10.1021/es970908y
Geelhoed, J.S., Hiemstra, T., Van Riemsdijk, W.H., 1997. Phosphate and sulfate adsorption on goethite: Single anion and competitive adsorption. Geochim. Cosmochim. Acta 61, 2389–2396. https://doi.org/10.1016/S0016-7037(97)00096-3

Gros, P., Ahmed, A., Kühn, O., Leinweber, P., 2017. Glyphosate binding in soil as revealed by sorption experiments and quantum-chemical modeling. Sci. Total Environ. 586, 527–535. https://doi.org/10.1016/j.scitotenv.2017.02.007
Gros, P., Ahmed, A.A., Kühn, O., Leinweber, P., 2019. Influence of metal ions on glyphosate detection by FMOC-Cl. Environ. Monit. Assess. 191. https://doi.org/10.1007/s10661-019-7387-2
Gu, Baohua., Schmitt, Juergen., Chen, Zhihong., Liang, Liyuan., McCarthy, J.F., 1994. Adsorption and desorption of natural organic matter on iron oxide: mechanisms and models. Environ. Sci. Technol. 28, 38–46. https://doi.org/10.1021/es00050a007
Guppy, C.N., Menzies, N.W., Moody, P.W., Blamey, F.P.C., 2005. Competitive sorption reactions between phosphorus and organic matter in soil: a review. Soil Res. 43, 189. https://doi.org/10.1071/SR04049
Gypser, S., Hirsch, F., Schleicher, A.M., Freese, D., 2018. Impact of crystalline and amorphous iron- and aluminum hydroxides on mechanisms of phosphate adsorption and desorption. J. Environ. Sci. 70, 175–189. https://doi.org/10.1016/j.jes.2017.12.001
Gypser, S., Schütze, E., Freese, D., 2021. Single and Binary Fe- and Al-hydroxides Affect Potential Phosphorus Mobilization and Transfer from Pools of Different Availability. Soil Syst. 5, 33. https://doi.org/10.3390/soilsystems5020033
Gypser, S., Schütze, E., Freese, D., 2019. Crystallization of single and binary iron- and aluminum hydroxides affect phosphorus desorption. J. Plant Nutr. Soil Sci. 182, 741–750. https://doi.org/10.1002/jpln.201700543
Han, J., Kim, M., Ro, H.-M., 2020. Factors modifying the structural configuration of oxyanions and organic acids adsorbed on iron (hydr)oxides in soils. A review. Environ. Chem. Lett. 18, 631–662. https://doi.org/10.1007/s10311-020-00964-4
Hongshao, Z., Stanforth, R., 2001. Competitive Adsorption of Phosphate and Arsenate on Goethite. Environ. Sci. Technol. 35, 4753–4757. https://doi.org/10.1021/es010890y
Jo, S., Kim, T., Iyer, V.G., Im, W., 2008. CHARMM-GUI: A web-based graphical user interface for CHARMM. J. Comput. Chem. 29, 1859–1865. https://doi.org/10.1002/jcc.20945
Johnson, S.E., Loeppert, R.H., 2006. Role of Organic Acids in Phosphate Mobilization from Iron Oxide. Soil Sci. Soc. Am. J. 70, 222. https://doi.org/10.2136/sssaj2005.0012
Kaiser, K., Guggenberger, G., 2003. Mineral surfaces and soil organic matter. Eur. J. Soil Sci. 54, 219–236. https://doi.org/10.1046/j.1365-2389.2003.00544.x
Kpomblekou-A, K., Tabatabai, M.A., 2003. Effect of low-molecular weight organic acids on phosphorus release and phytoavailabilty of phosphorus in phosphate rocks added to soils. Agric. Ecosyst. Environ. 100, 275–284. https://doi.org/10.1016/S0167-8809(03)00185-3
Kruse, J., Abraham, M., Amelung, W., Baum, C., Bol, R., Kühn, O., Lewandowski, H., Niederberger, J., Oelmann, Y., Rüger, C., Santner, J., Siebers, M., Siebers, N., Spohn, M., Vestergren, J., Vogts, A., Leinweber, P., 2015. Innovative methods in soil phosphorus research: A review. J. Plant Nutr. Soil Sci. 178, 43–88. https://doi.org/10.1002/jpln.201400327
Kubicki, J.D. (Ed.), 2016. Molecular modeling of geochemical reactions: an introduction. Wiley, Chichester, West Sussex, United Kingdom.
Kubicki, J.D., Ohno, T., 2020. Integrating Density Functional Theory Modeling with Experimental Data to Understand and Predict Sorption Reactions: Exchange of Salicylate for Phosphate on Goethite. Soil Syst. 4, 27. https://doi.org/10.3390/soilsystems4020027
Kubicki, J.D., Paul, K.W., Kabalan, L., Zhu, Q., Mrozik, M.K., Aryanpour, M., Pierre-Louis, A.-M., Strongin, D.R., 2012. ATR-FTIR and density functional theory study of the structures, energetics, and vibrational spectra of phosphate adsorbed onto goethite. Langmuir ACS J. Surf. Colloids 28, 14573–14587. https://doi.org/10.1021/la303111a
Langmuir, I., 1918. The adsorption of gases on plane surfaces of glass, mica and platinum. J. Am. Chem. Soc. 40, 1361–1403. https://doi.org/10.1021/ja02242a004
Leinweber, P., Schulten, H.-R., 1999. Advances in analytical pyrolysis of soil organic matter. J. Anal. Appl. Pyrolysis 49, 359–383. https://doi.org/10.1016/S0165-2370(98)00082-5
Liu, Q., Guo, L., Zhou, Y., Dai, Y., Feng, L., Zhou, J., Zhao, J., Liu, J., Qian, G., 2012. Phosphate adsorption on biogenetic calcium carbonate minerals: effect of a crystalline phase. Desalination Water Treat. 47, 78–85. https://doi.org/10.1080/19443994.2012.696798
Liu, X., Tournassat, C., Grangeon, S., Kalinichev, A.G., Takahashi, Y., Marques Fernandes, M., 2022. Molecular-level understanding of metal ion retention in clay-rich materials. Nat. Rev. Earth Environ. 3, 461–476. https://doi.org/10.1038/s43017-022-00301-z
Luengo, C., Brigante, M., Antelo, J., Avena, M., 2006. Kinetics of phosphate adsorption on goethite: comparing batch adsorption and ATR-IR measurements. J. Colloid Interface Sci. 300, 511–518. https://doi.org/10.1016/j.jcis.2006.04.015

Maciá, E., 2005. The role of phosphorus in chemical evolution. Chem. Soc. Rev. 34, 691. https://doi.org/10.1039/b416855k
Minamisawa, H., Kojima, Y., Aizawa, M., 2022. Adsorption of Inositol Phosphate on Hydroxyapatite Powder with High Specific Surface Area. Materials 15, 2176. https://doi.org/10.3390/ma15062176
Negassa, W., Dultz, S., Schlichting, A., Leinweber, P., 2008. Influence of specific organic compounds on phosphorus sorption and distribution in a tropical soil. Soil Sci. 173, 587–601. https://doi.org/10.1097/SS.0b013e3181847eef
Norén, K., Persson, P., 2007. Adsorption of monocarboxylates at the water/goethite interface: The importance of hydrogen bonding. Geochim. Cosmochim. Acta 71, 5717–5730. https://doi.org/10.1016/j.gca.2007.04.037
Ognalaga, M., Frossard, E., Thomas, F., 1994. Glucose-1-phosphate and Myo-inositol Hexaphosphate Adsorption Mechanisms on Goethite. Soil Sci. Soc. Am. J. 58, 332–337. https://doi.org/10.2136/sssaj1994.03615995005800020011x
Okano, K., Uemoto, M., Kagami, J., Miura, K., Aketo, T., Toda, M., Honda, K., Ohtake, H., 2013. Novel technique for phosphorus recovery from aqueous solutions using amorphous calcium silicate hydrates (A-CSHs). Water Res. 47, 2251–2259. https://doi.org/10.1016/j.watres.2013.01.052
Osman, A.I., Zhang, Y., Lai, Z.Y., Rashwan, A.K., Farghali, M., Ahmed, A.A., Liu, Y., Fang, B., Chen, Z., Al-Fatesh, A., Rooney, D.W., Yiin, C.L., Yap, P.-S., 2023. Machine learning and computational chemistry to improve biochar fertilizers: a review. Environ. Chem. Lett. 21, 3159–3244. https://doi.org/10.1007/s10311-023-01631-0
Ozboyaci, M., Kokh, D.B., Corni, S., Wade, R.C., 2016. Modeling and simulation of protein–surface interactions: achievements and challenges. Q. Rev. Biophys. 49. https://doi.org/10.1017/S0033583515000256
Rakovan, J., Becker, U., Hochella, M.F., 1999. Aspects of goethite surface microtopography, structure, chemistry, and reactivity. Am. Mineral. 84, 884–894. https://doi.org/10.2138/am-1999-5-623
Roy, E.D., Willig, E., Richards, P.D., Martinelli, L.A., Vazquez, F.F., Pegorini, L., Spera, S.A., Porder, S., 2017. Soil phosphorus sorption capacity after three decades of intensive fertilization in Mato Grosso, Brazil. Agric. Ecosyst. Environ. 249, 206–214. https://doi.org/10.1016/j.agee.2017.08.004
Ruttenberg, K.C., Sulak, D.J., 2011. Sorption and desorption of dissolved organic phosphorus onto iron (oxyhydr)oxides in seawater. Geochim. Cosmochim. Acta 75, 4095–4112. https://doi.org/10.1016/j.gca.2010.10.033
Shaheen, S.M., Wang, J., Baumann, K., Ahmed, A.A., Hsu, L.-C., Liu, Y.-T., Wang, S.-L., Kühn, O., Leinweber, P., Rinklebe, J., 2022. Stepwise redox changes alter the speciation and mobilization of phosphorus in hydromorphic soils. Chemosphere 288, 132652. https://doi.org/10.1016/j.chemosphere.2021.132652
Sibanda, H.M., Young, S.D., 1986. Competitive adsorption of humus acids and phosphate on goethite, gibbsite and two tropical soils. J. Soil Sci. 37, 197–204. https://doi.org/10.1111/j.1365-2389.1986.tb00020.x
Strauss, R., Brümmer, G.W., Barrow, N.J., 1997a. Effects of crystallinity of goethite: I. Preparation and properties of goethites of differing crystallinity. Eur. J. Soil Sci. 48, 87–99. https://doi.org/10.1111/j.1365-2389.1997.tb00188.x
Strauss, R., Brummer, G.W., Barrow, N.J., 1997b. Effects of crystallinity of goethite: II. Rates of sorption and desorption of phosphate. Eur. J. Soil Sci. 48, 101–114. https://doi.org/10.1111/j.1365-2389.1997.tb00189.x
Tejedor-Tejedor, M.I., Anderson, M.A., 1990. The protonation of phosphate on the surface of goethite as studied by CIR-FTIR and electrophoretic mobility. Langmuir 6, 602–611. https://doi.org/10.1021/la00093a015
Tisdale, S.L., Tisdale, S.L. (Eds.), 1993. Soil fertility and fertilizers, 5th ed. ed. Prentice Hall, Upper Saddle River, N.J.
Tsao, T.M., Chen, Y.M., Wang, M.K., 2011. Origin, separation and identification of environmental nanoparticles: a review. J. Environ. Monit. 13, 1156. https://doi.org/10.1039/c1em10013k
Tunesi, S., Poggi, V., Gessa, C., 1999. Phosphate adsorption and precipitation in calcareous soils: the role of calcium ions in solution and carbonate minerals. Nutr. Cycl. Agroecosystems 53, 219–227. https://doi.org/10.1023/A:1009709005147
Urrutia, O., Guardado, I., Erro, J., Mandado, M., García-Mina, J.M., 2013. Theoretical chemical characterization of phosphate-metal-humic complexes and relationships with their effects on both phosphorus soil fixation and phosphorus availability for plants: Theoretical chemical

characterization of phosphate-metal-humic complexes. J. Sci. Food Agric. 93, 293–303. https://doi.org/10.1002/jsfa.5756
Van Der Spoel, D., Lindahl, E., Hess, B., Groenhof, G., Mark, A.E., Berendsen, H.J.C., 2005. GROMACS: Fast, flexible, and free. J. Comput. Chem. 26, 1701–1718. https://doi.org/10.1002/jcc.20291
Wang, H., Zhu, J., Fu, Q., Hong, C., Hu, H., Violante, A., 2016. Phosphate adsorption on uncoated and humic acid-coated iron oxides. J. Soils Sediments 16, 1911–1920. https://doi.org/10.1007/s11368-016-1383-8
Wang, H., Zhu, J., Fu, Q., Hu, H., 2015a. Adsorption of phosphate on pure and humic acid-coated ferrihydrite. J. Soils Sediments 15, 1500–1509. https://doi.org/10.1007/s11368-015-1095-5
Wang, H., Zhu, J., Fu, Q.-L., Xiong, J.-W., Hong, C., Hu, H.-Q., Violante, A., 2015b. Adsorption of Phosphate onto Ferrihydrite and Ferrihydrite-Humic Acid Complexes. Pedosphere 25, 405–414. https://doi.org/10.1016/S1002-0160(15)30008-4
Wang, Y.T., Zhang, T.Q., O'Halloran, I.P., Tan, C.S., Hu, Q.C., 2016. A phosphorus sorption index and its use to estimate leaching of dissolved phosphorus from agricultural soils in Ontario. Geoderma 274, 79–87. https://doi.org/10.1016/j.geoderma.2016.04.002
Weng, L., Van Riemsdijk, W.H., Hiemstra, T., 2008. Humic Nanoparticles at the Oxide−Water Interface: Interactions with Phosphate Ion Adsorption. Environ. Sci. Technol. 42, 8747–8752. https://doi.org/10.1021/es801631d
Werdin-Pfisterer, N.R., Kielland, K., Boone, R.D., 2012. Buried organic horizons represent amino acid reservoirs in boreal forest soils. Soil Biol. Biochem. 55, 122–131. https://doi.org/10.1016/j.soilbio.2012.06.012
Westergaard Strobel, B., Bernhoft, I., Borggaard, O.K., 1999. Low-molecular-weight aliphatic carboxylic acids in soil solutions under different vegetations determined by capillary zone electrophoresis. Plant Soil 212, 115–121. https://doi.org/10.1023/A:1004637126429
Yan, J., Jiang, T., Yao, Y., Lu, S., Wang, Q., Wei, S., 2016. Preliminary investigation of phosphorus adsorption onto two types of iron oxide-organic matter complexes. J. Environ. Sci. 42, 152–162. https://doi.org/10.1016/j.jes.2015.08.008
Yan, Y.P., Liu, F., Li, W., Liu, F., Feng, X.H., Sparks, D.L., 2014. Sorption and desorption characteristics of organic phosphates of different structures on aluminium (oxyhydr)oxides: Sorption-desorption of organic P on Al oxyhydroxides. Eur. J. Soil Sci. 65, 308–317. https://doi.org/10.1111/ejss.12119
Zhong, B., Stanforth, R., Wu, S., Chen, J.P., 2007. Proton interaction in phosphate adsorption onto goethite. J. Colloid Interface Sci. 308, 40–48. https://doi.org/10.1016/j.jcis.2006.12.055